To the Graduate Council:

I am submitting herewith a thesis written by Abdallah Jubran Jubran entitled "Finite Element Analysis of Behavior of AISC Standard Type II Connections." I recommend that it be accepted in partial fulfillment of the requirements for the degree of Master of Engineering, with a major in Civil Engineering.

David W. Goodpasture

David W. Goodpasture, Major Professor

We have read this thesis and recommend its acceptance:

John E Akin

Edwin G. Burdette

Accepted for the Council:

L Evans Roth

Vice Chancellor
Graduate Studies and Research

FINITE ELEMENT ANALYSIS OF BEHAVIOR OF AISC STANDARD TYPE II CONNECTIONS

A Thesis

Presented for the

Master of Engineering

Degree

The University of Tennessee, Knoxville

Abdallah Jubran Jubran

June 1981

ACKNOWLEDGMENTS

The author wishes to express special appreciation to Dr. David Goodpasture for his guidance and suggestions which contributed to this thesis.

The author also acknowledges Dr. Edwin Burdette who served on the graduate committee and assisted in the review of the manuscript.

Special thanks are due to Dr. John E. Akin who served on the graduate committee, provided valuable modeling hints, and provided unlimited access to the finite element computer code used in this research.

Gratitude is expressed to Mr. Ramzi Abdul-Ahad for his advice and encouragement, and to Mrs. Maxine Martin for her assistance in typing.

Finally, the author expresses deep appreciation to his family for their constant encouragement, support and enthusiasm during his study at The University of Tennessee, Knoxville.

ABSTRACT

The first purpose of this study was to obtain a theoretical elastic behavior of three AISC standard framed beam connections (Type 2). The finite element method was used for predicting this behavior. Most elements were eight noded quadrilaterals. Those elements were used for the angle as well as the beam web. Other types of elements used were spring elements for modeling the bolts that frame the connection into the column, and six-noded elements for modeling the beam flange.

The second purpose of this study was to compare the behavior predicted by finite element analysis to the results of tests on the same connections and to the behavior as predicted by theoretical design equations.

A comparison was made of the following characteristics: yield moment and yield rotation. The comparison showed that the yield moments obtained from finite element results were consistently higher than either observed or predicted values. It was also shown that the yield rotations were larger than predicted yield rotations consistently, and larger than experimentally observed values for two of the three angle thicknesses considered. It was concluded that computer results were sensitive to connection boundary conditions.

TABLE OF CONTENTS

LIST OF FIGURES

FIGURE PAGE

CHAPTER I

INTRODUCTION

The American Institute of Steel Construction (AISC) recognizes in its current specifications three types of structural connections (14). Those are:

AISC Type 1: Rigid Frame Connections

AISC Type 2: Simple Framing Connections

AISC Type 3: Semirigid Framing Connections

The difference in the three types is the amount of moment transfer between connecting members. For Type 1 connections full continuity is provided at the connection so that the original angles between intersecting members are held virtually constant. Stated differently, the rotational restraint is of the order of 90 percent or more of that needed to prevent any angle change (20). For Type 2 connections, the rotational restraint is as little practicable, or the original angle between intersecting members may change up to 80 percent of the amount it would theoretically change if frictionless hinged connections were used instead (20). Those are two extreme connection types, and design assumptions are to consider only shear transfer (no moment) at the ends for simple framings, and full moment transfer for rigid frame connections. Type 3 semirigid connections are intermediate in moment transfer. Connections may be considered to be semirigid if the rotational restraint they provide is between 20 and 90 percent of that necessary to prevent any relative angle change between the beam end and the column (20). AISC § 1.2 states that design using Type 3 connections can be done when "the connections of beams and girders possess a dependable and known moment capacity intermediate in degree between the rigidity of Type 1 and the flexibility of Type 2" (14).

Type 3 connections are least used in designs although economy may be achieved by using them. The lack of information to predict the behavior of such connections is the singlemost important factor in their limited use. The purpose of this study is to compare the elastic behavior of such connections as obtained by a finite element investigation to observed behavior of the same connections. For three clip angle beam column connections the following are reported here: yield moment, yield rotation, principal stresses, in plane shearing stress, effective stress, as well as plots showing the displaced shape of the structure and variation of displacements along selected nodal lines.

CHAPTER II

REVIEW OF THE LITERATURE

I. HISTORICAL BACKGROUND

The behavior of bolted connections has been a subject of the investigation that has been given a lot of emphasis by structural engineers. This is due mainly to the presence of high-strength bolts as a connecting medium. It is the introduction of the high-strength bolt as a structural connector that has made it possible to produce structural joints that are superior to and often more economical than comparable riveted joints (15).

Batho and Bateman, in 1934, first reported the possibility of using high-strength bolts in steel-framed construction. They concluded that bolts with a minimum yield strength of 54 KSI could be relied on to prevent slippage of connected parts (20). In 1938, W. M. Wilson conducted tests on high-strength bolts. His findings further substantiated Batho's conclusions. Wilson concluded that if high-strength bolts were tightened sufficiently to eliminate slip in a structural joint then the bolts did not fail due to fatigue. Wilson's findings gave the initial impetus for further research (15). In 1947 a Research Council on riveted and bolted structural joints was formed and began a number of studies at The University of Illinois, Urbana, on joints assembled with high-strength bolts (15). Since then the Research Council has continued to organize and sponsor research on high-strength bolted connections, and issue specifications at intervals on the basis of research findings (20).

In 1948 The American Railway Engineering Association also became interested in bolted connections. In the same year, The Association of American Railroads started a number of field test installations which confirmed the adequacy of high-strength bolted connections (10).

Replacement of rivets by high-strength bolts on a one-to-one basis was allowed in the first specifications of the Research Council in 1951 (20).

II. TYPES OF CONNECTIONS

The American Institute of Steel Construction (AISC) recognizes in its current specifications three types of structural connections (14). Those are:

AISC Type 1: Rigid Frame Connections

AISC Type 2: Simple Framing Connections

AISC Type 3: Semirigid Framing Connections

The difference in the three types is the amount of moment transfer between connecting members. For Type 1 connections full continuity is provided at the connection so that the original angles between intersecting members are held virtually constant. Stated differently, the rotational restraint is of the order of 90 percent or more of that needed to prevent any angle change (20). For Type 2 connections, the rotational restraint is as little as practicable, or the original angle between intersecting members may change up to 80 percent of the amount it would theoretically change if frictionless hinged connections were used instead (20). Those are two extreme connection types, and design assumptions are to consider only shear transfer (no moment) at the ends for simple framings, and full moment transfer for rigid frame connections. Type 3 semi-rigid connections are intermediate in moment transfer. Connections may be considered to be semi-rigid if the rotational restraint they provide is between 20 and 90 percent of that necessary to prevent any relative angle change between the beam end and the column (20). Munse et al. used (Ref. 16) the term "per cent rigidity" as a measure of restraint at the end of the beam. In that paper, the authors define this as the ratio of the moments developed at the ends due to a loading condition to the fixed-end moment that would exist under the same loading. Thus, we can say that Type 1 connections possess a rigidity of 90 percent or more; Type 2 connections have a 20 percent rigidity or less; and Type 3 semi-rigid framing connections as having a percent rigidity between 20 and 90. AISC § 1.2 states that design using Type 3 connections can be done when "the connections of beams and girders possess a dependable and known moment capacity intermediate in degree between the rigidity of Type 1 and the flexibility of Type 2" (14). Driscoll (Ref. 3) states that "information that is available on semi-rigid connections is usually limited to joints that are compact in length, so that only moment-rotation characteristics are considered." Krishnamurthy and co-workers (Ref. 10) state that moment-rotation relationships are needed in the following situations involving bolted moment-resistant connection, "(1) in the design of semi-rigid connections with limiting deflection, drift, or rotation considerations; and (2) in the analysis of 'rigid' frames with non-rigid connections." The term rotation, denoted by ϕ, is the rotation of the beam relative to the column (10). This is also the definition adapted by Munse, Bell and Chesson in Ref. 16.

A moment-rotation diagram is shown in Figure 1. The axis of abscissae is the axis of rotations, ϕ, while the axis of ordinates is the axis of moments. The vertical axis has $\phi = 0$, and therefore represents the ideal rigid frame (or moment resistant) connection, whereas the horizontal axis has $M = 0$, and represents the other extreme case of the frictionless hinged (or shear) connection. See Figure 1.

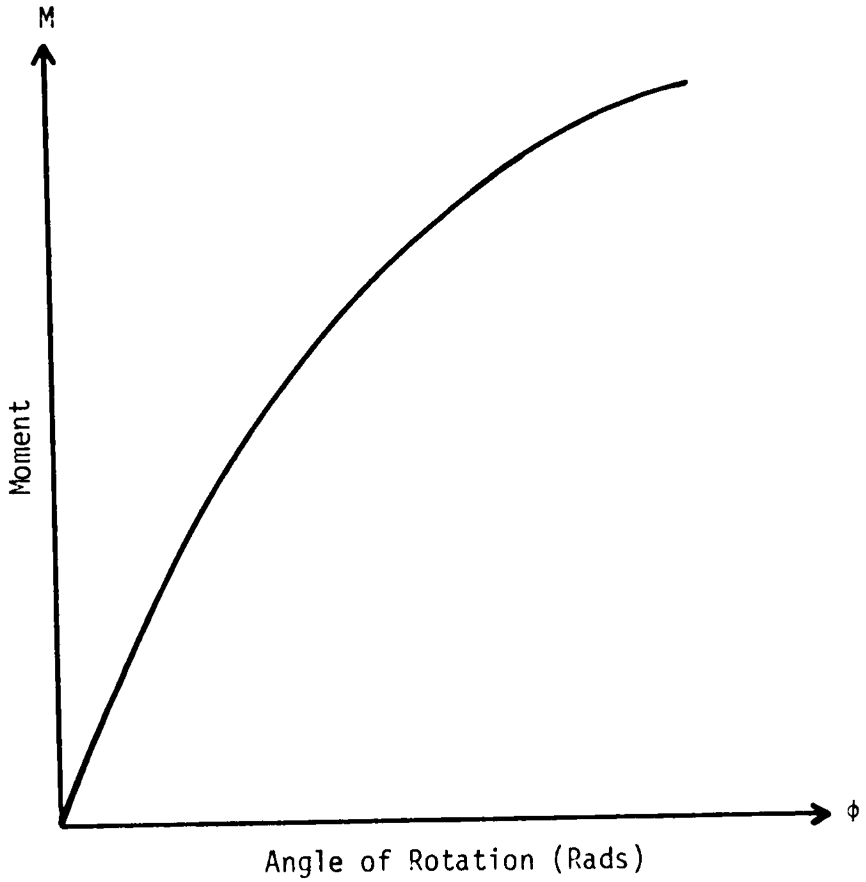

Figure 1. Typical Moment-Rotation (M-ϕ) Curve.

Beam column connections are important in structural frames, as they partition the loads (5). As stated before, simple connections transfer end reactions of beams to columns. If restraints are provided, beam end rotations are minimized, and the maximum positive moment in the beam can be reduced by the resulting end moments (5). So, beam end rotations are only minimized, not eliminated as assumed for design purposes. Figure 2, adapted from Reference 5, shows typical moment rotation curves for different connections, as well as a typical beam-line.

III. SIGNIFICANT RESEARCH

Bolted connections received widespread acceptance by structural engineers and led to the eventual obsolescence of their riveted counterparts.

Numerous studies have been conducted to study the behavior of such connections. In a 1956 A.S.C.E. Transactions paper, Munse summarized research on bolted connections (15). His summary cites economy as an important reason for the general acceptance of such connections. A necessary condition for obtaining full benefit from their use is that the connections be installed with a high initial tension or simply a pre-tension. This pretension of at least 90 percent of the proof load of the bolts leads to superior performance by way of eliminating slip through friction between the connected parts. This is the means that riveted connections resisted working loads, although their design was based on the premise that the loads were transferred by direct shear on the rivets. To develop the frictional resistance of high strength bolts under working load conditions, a high axial tension (pretension) must be

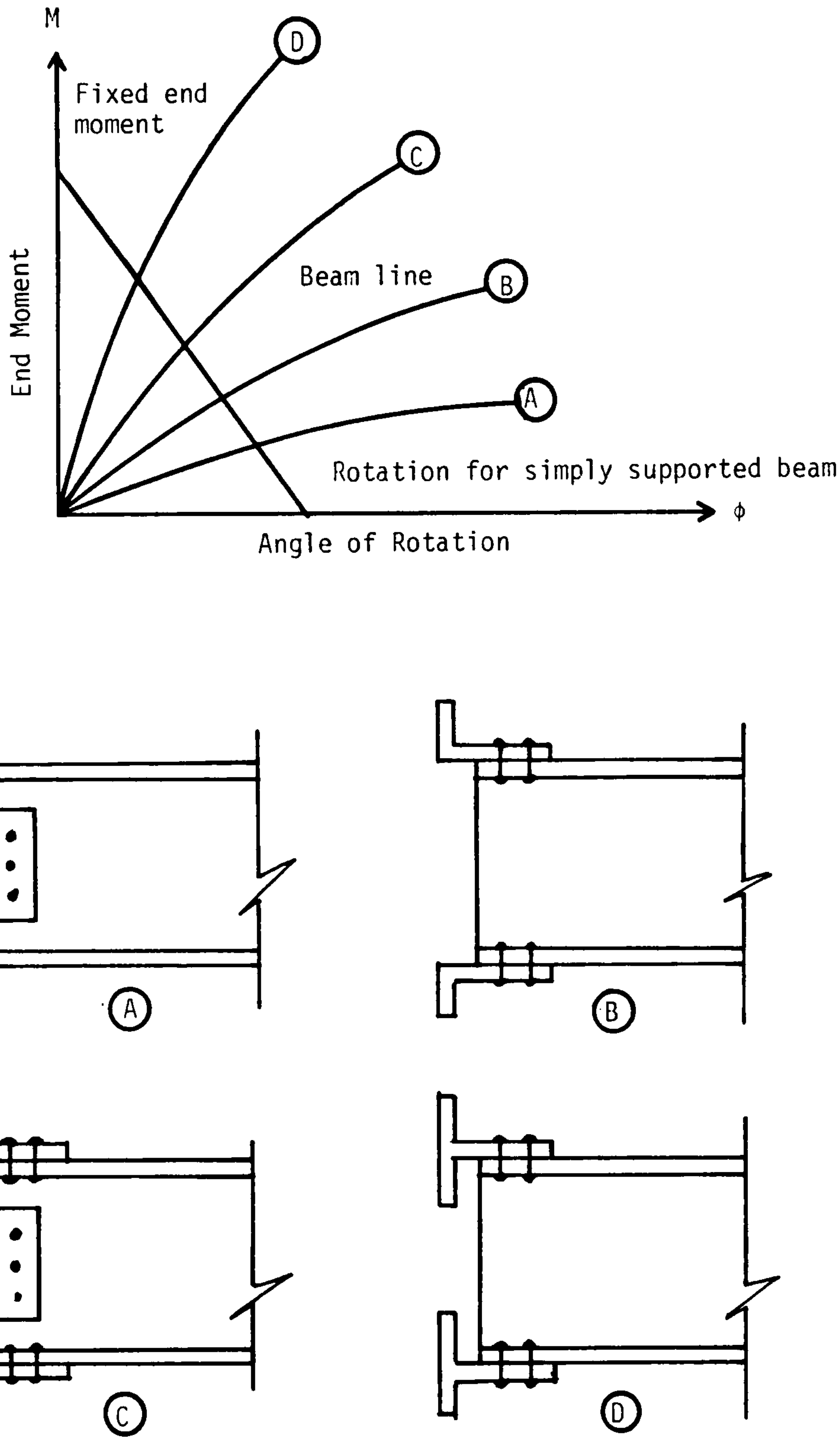

Figure 2. M-ϕ Curves for Four Types of Connections.

maintained at all times. This pretension, as stated before, should be at least 90 percent of the bolt proof load.

Munse and Chesson summarized results of a series of tests that were conducted at the University of Illinois. Their test results were described in an ASCE Proceedings paper in 1959 (16). Their experiments were on simple beam connections or shear connections, and showed that beam-column connections actually do provide some end restraint to rotation. The test results also revealed that this end restraint increases slightly by the use of high strength bolts in lieu of rivets for fastening the flanges of the column and connection angles together. With bolts properly tightened, a high clamping force was developed in heat treated high-strength bolts. This clamping force can be developed with any bolt length, resulting in a high tension (pretension) approximately twice that of rivets as a result of shrinkage during cooling. Munse and Chesson used four specimens, three bolted and one riveted. One specimen was loaded to the capacity of the testing machine and did not fail, while the other three experienced tearing of the angle on the tension side. This tearing resulted primarily from bending, although all connections were subjected to both moment and shear. The percent rigidity ratios varied from 7.6 percent for the riveted connection to 12.6 percent. The moment-rotation characteristics were as follows. "At low loads (moments up to 200 in. Kips) the rotation of the beams was approximately proportional to the connection moment. Then, as the connection angles began to yield, the rotation increased in a non-linear manner with respect to the applied moment; however as the moment was increased still further, the rotation assumed a new linear variation with moment and continued this behavior up to the maximum moment for which the rotation readings were taken" (15). The approximately proportional response in the early loading stages observed by many authors is attributable to many factors amongst which is the unknown residual stress distribution present.

Recent research has been mainly concerned with prying forces that develop in bolts. Douty and McGuire addressed this problem in 1965. They suggested prying force formulas based on their research. Nair, et al. in 1974, suggested formulas based on their work on tee hangers (17). In 1976, Agerskov suggested some other formulas based on his research. Those versions are basically the same with adjusted coefficients to reflect individual test results (9). According to Nair et al. the deformation of connected parts in tee hanger connections could produce an increase in the tensile load on the fasteners, a phenomenon called prying action. This reduces both the ultimate load capacity and fatigue strength in the connections (17). In addition to the experimental investigation of tee-hangers, Nair, Birkemoe and Munse studied the same connections analytically using the finite element method. They considered steel as an elastic, perfectly plastic (no strain hardening) material. The elements used were plane stress elements, and bending parallel to the web was neglected (17).

As the finite element method became more popular, researchers in behavior of connections began using it as an analysis method to compare with experimental studies, as evidenced in the preceding paragraph.

Krishnamurthy and co-workers at Auburn University, and later at Vanderbilt University, followed this approach. Their research is related to end plate connections. In their investigation, thirteen bench-mark connections, having commonly used dimensions, were analyzed in two manners. First, as three-dimensional problems and second as two dimensional or in-plane problems. The object behind such an investigation was to obtain correlation factors between the full three-dimensional analysis and the simplified two-dimensional version. The correlation factors obtained were later used in subsequent research to predict the actual three dimensional behavior from the simpler and less expensive two-dimensional response as reflected in the results of the in-plane analysis (8, 9, 10). Also, Krishnamurthy presents an analytical study of moment rotation curves (Ref. 10) based on convergence studies. Quadrilateral elements were used with non-linear material capabilities. An idealized stress-strain behavior of steel was represented an an elastic-perfectly plastic bilinear variation.

A parameter study was also conducted with various "PI" terms (or groups of non-dimensional combinations of variables). The parameter investigation was based on sensitivity studies. The work of Krishnamurthy et al. can be extended to study the behavior of different bolted connections (10).

IV. LOTHERS' DERIVATIONS

In simply supported beams the entire moment diagram, when plotted on the compression side, is above the line representing the beam. For fixed-ended beams, the moment diagram falls both above and below the beam line. The larger moment for fixed-ended beams usually occurs at the end and controls the design. For symmetrical loading of simple beams, the centerline moment is the design moment. If the end-restraints are allowed to yield somewhat through some rotation ϕ, the above mentioned extreme situations could be avoided. This rotation ϕ is the additional rotation of beam over that of the column due to the deformation of the angle. If the end-restraints are allowed to yield enough, there will be a rotation ϕ_D such that both maximum positive and maximum negative bending moments become equal in magnitude and this moment value controls the design. This can be achieved through an appropriately designed semi-rigid connection. A connection so designed is more economical, and the column resists a smaller moment (13).

Lothers (Ref. 13) follows a rationale that leads to the design of semi-rigid connections. He introduced a factor, the semi-rigid connection factor, needed before any design can be carried out (13). This factor is denoted by Z. Driscoll calls Z the flexibility coefficient (3). Z is given by the following equation

$$Z = \frac{\phi}{M} \qquad 1(a)$$

or alternatively

$$\phi = MZ \qquad 1(b)$$

where

M is the moment at the end of beam due to applied load(s), and ϕ is the additional angular rotation of the beam over that of column due to deformation of the angle, also known as the angle of strain (13). This is shown in Figure 3 (Figure 802 of Ref. 13), and compared with a rigid connection ($\phi = 0$).

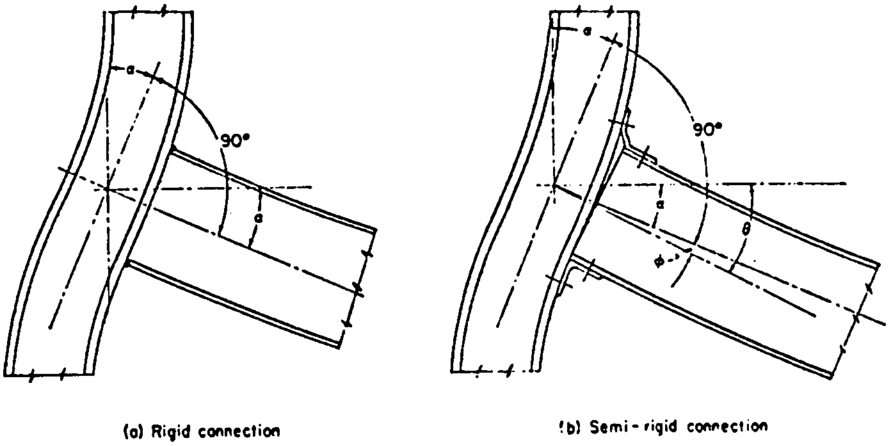

Figure 3. Comparison between Rigid and Semirigid Connections.
Source: Ref. 14, Ch. 8.

Z can be determined from experimental moment-rotation (M - ϕ) curves or "connection curves" (10). It can also be determined analytically as Lothers does for Type A web-angle connections where equations for ϕ and M are derived in terms of known quantities and properties. The work can be extended to other type connections. It is to be noted that the Z value obtained is for a particular connection only (13). There are two simplifications used in deriving the analytical expressions. The first is that there is an abrupt angle change ϕ, occurring at the end of the beam (13). The second is that no previous loading history or residual stresses are accounted for (13, 19). Lothers' reasoning is logical and valid for the elastic response of the angle which is the usual design range.

The angle of strain will be defined, for our purposes, as follows:

$$\phi = \frac{\Delta}{h} \tag{2}$$

where Δ is the relative x-displacement of top and bottom ends of the beam end, and h is the height of the beam. ϕ is given by a similar equation in Reference 13. This is shown in Figure 4 below.

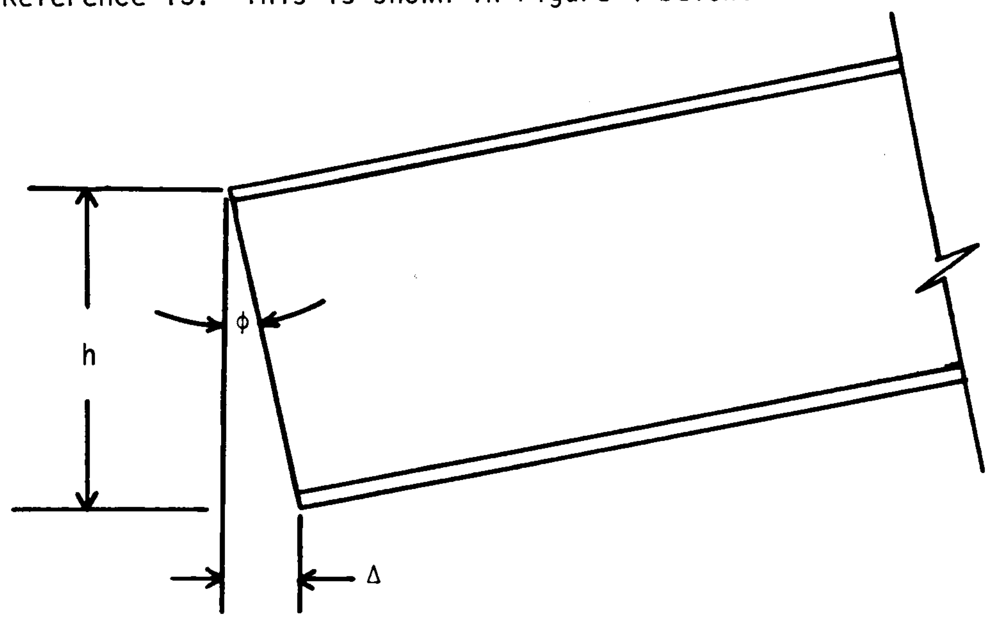

Figure 14. Beam-End Measurement of Rotation.

The angle of strain ϕ at an end of a beam depends on the moment M at the same end. ϕ increases when M is increased. However, the connection stiffness entirely governs this increase (13). The connection response is inherently non-linear in character (10). In the early loading stages the behavior may be stiffened to a nearly linear response due to bolt pretensioning. An initially linear response was obtained experimentally by Munse in 1959. Thus the flexibility coefficient Z must be carefully and judiciously determined from experimental curves, as such curves do not possess a substantial straight line portion (3). Driscoll states that, "Lothers' theoretical curves agree well with initial slope of experimental moment-rotation curves by Rathbun." Lothers also defines Z as a correction factor when used with E and I of the beam rendering applicable, usual, exact methods (such as moment distribution) (13). Lothers shows that for a semi-rigidly connected beam, the equivalent length of a fixed ended beam for moment distribution is

$$L_{EQ} = L + 3EIZ \tag{3}$$

Also for aunit value of M, $Z = \phi$. Thus when axial effects are neglected, Z is equal to the joint rotation (3).

CHAPTER III

REVIEW OF THE FINITE ELEMENT METHOD

I. BRIEF HISTORY

The origins of the finite element method date back to the early 1940's (7). The method made its first appearance in the 1950's as a solution technique associated with solid mechanics problems (21). R. Clough was the first to utilize the name "finite element method" in a paper on two-dimensional elasticity in 1960 (7). The term "finite element method" was used in reference to subdividing a system under consideration into simpler subsystems or elements. Since then, the method has grown in both theory and application. Its theory at first lacked its present mathematical rigor (1). With its theoretical and mathematical aspects better understood, the finite element method has become an important tool for numerical analysis with a wide range of applications in the various engineering disciplines as well as the physical and the applied sciences (1).

In what follows, the focus will be on the application of the method to problems of structural analysis.

II. MATRIX METHOD AND FINITE ELEMENT APPROACH IN STRUCTURAL ANALYSIS

The finite element and the matrix method are two approaches that can be resorted to in analyzing structural systems with complex behavior (12). Each method is well suited for situations where the assumptions used in deriving its equations are valid.

The ordinary matrix method is suitable when truss type or frame type structures are being considered. It fails, however, in situations where "deep beams," or beams with shear, are involved. This is because shear stresses become significant and the stress distribution over the cross-section is not that assumed in simple beam theory. In such cases as well as in plate type, shell type and axisymmetric structures, the finite element method becomes a powerful tool. The method is capable of handling a wide variety of problems with various complexities. It is capable of handling two-dimensional as well as three-dimensional problems of stress analysis in the elastic as well as the inelastic stage. The material could be isotropic, homogeneous, inhomogeneous, as well as composite. The finite element method is considered an outgrowth of the traditional displacement based matrix approach made suitable for multi-dimensional problems where a continuous distribution of the variable of interest exists (2, 21).

III. STANDARD ANALYSIS PROCEDURE

There is a solution methodology applicable to all continuum problems, analyzed by the finite element method, irrespective of its nature or dimension. This process is outlined below showing the sequence of steps in their proper order (1, 2, 7, 21, 22).

1. Discretize the solution domain Ω.
2. Describe behavior of a typical element.
3. Assemble system equations and apply boundary condition to reflect overall system behavior.
4. Solve system equations.
5. Post solution calculations.

In what follows, each of the preceding steps will be dealt with in more detail.

Discretization

The system under consideration, over a domain Ω, is subdivided into a number (finite) of smaller subdomains Ω^e, or elements, as shown in Figure 5. Since the actual system possesses a complex behavior, individual element behavior is more readily understood (7). Those elements are separated by imaginary lines (or planes) which define the boundaries, Γ^e, of the element, also called nodal lines or nodal planes (see Figure 5).

The elements are assumed to be interconnected at a specified number of points called nodes (see Figure 5). Nodes are analogous to joints in structural analysis (2). Nodes can be situated anywhere in the element, usually at the boundaries and, in certain problems, inside the element. This is the choice of the analyst. Nodes are allowed degrees of freedom compatible with the degrees of freedom, or parameters, of the system. In structural applications, nodal parameters are displacements, slopes, and curvatures (or generalized displacements). The displacements are the basic unknowns sought for in the solution; they specify uniquely and simultaneously the element and system behavior (1, 6, 22).

Typical Element Description

To fully describe an element behavior we need to know the following:

1. How an element deforms.
2. A Strain-displacement relation.

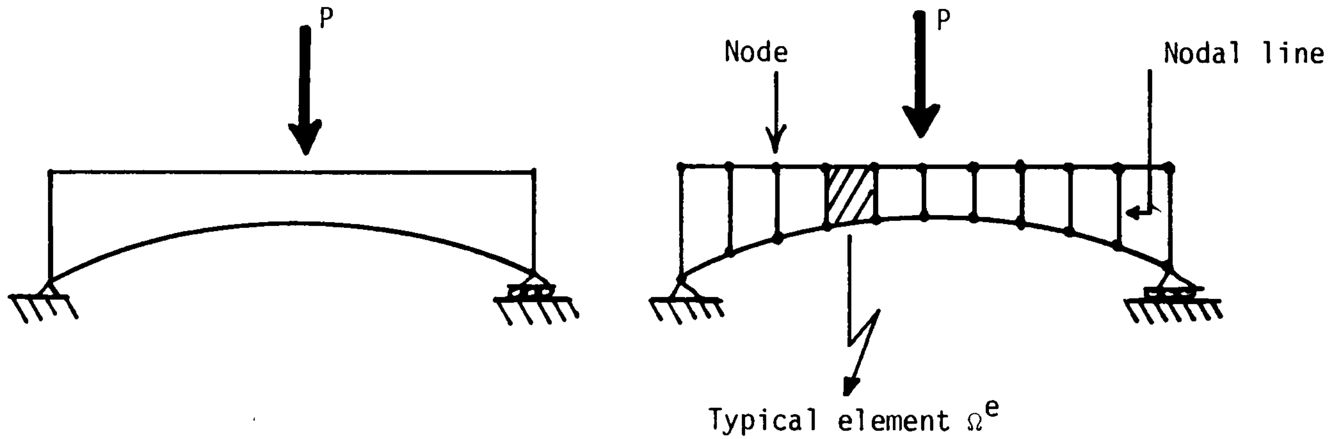

a. Standard system

b. Discretized system

Figure 5. Comparison between Standard and Discrete Systems.

3. A stress-strain relation.

4. Structure and/or element equilibrium equations.

<u>Element deformation</u>. As stated before for a finite element model, elements comprising the whole system are assumed to be connected along their boundaries at discrete points called nodes. Displacements in a typical element are assumed to be a function of the element nodal displacements (2). The displacement in each element will be expressed in terms of nodal displacements and interpolation functions as follows:

$$[U]^T = \sum N_i u_i \quad . . . \tag{4}$$

where

U = displacement vector

N_i = interpolation function for node i

u_i = displacement of node i

The functions N_i, provide an approximation to the actual behavior of the unknown parameter u_i over an element. Interpolation functions are also called shape functions, approximation functions and field variable models. These provide a piecewise approximation for the whole solution domain, Ω (7). In general, the solution obtained, regardless of the fineness of subdivision is only approximate because the infinite number of degrees of freedom of the system are limited by the assumed shape functions. However, in some special cases only the exact solution is obtained indeed by a limited number of subdivisions. This is the case when the correct solution is fitted exactly by the assumed solution (22). Such a case occurs for example in the analysis of beams where an analytical solution is known, and is a polynomial of some order, n. If assumed shape functions are polynomials of order n, then the analytic and finite element solutions are the same. Polynomials are almost exclusively used for shape functions. They are easily integrated and differentiated. Also local sections of continuous functions can be thought of as truncated Taylor series expansions (21).

As an example of interpolation functions, consider the following linear element e shown in Figure 6 below.

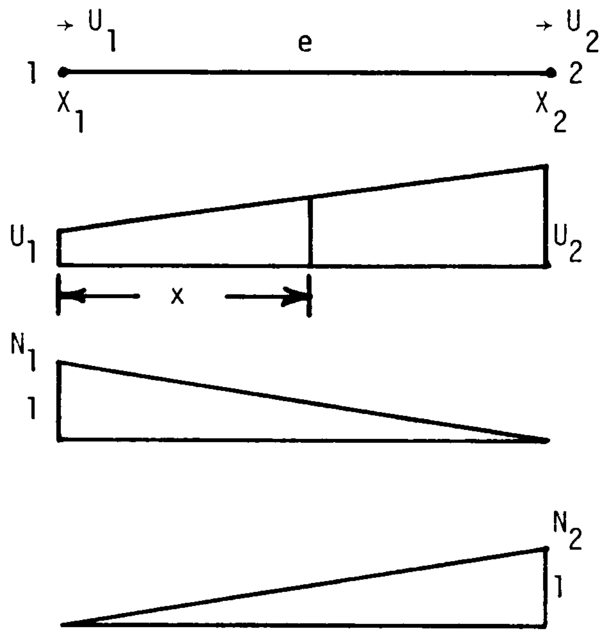

Figure 6. Linear Element Showing Variation of Variable U and Its Interpolation Functions.

Element e connects nodes 1 and 2, with variable U taking the values U_1 and U_2 at nodes 1 and 2 respectively. To determine U^e at any point within e using Equation 4, we do the following:

$$U^e(x) = \sum N_i u_i$$
$$= N_1U_1 + N_2U_2$$

At $x = x_1$ $\quad U^e(x) = U_1$

and at $x = x_2$ $\quad U^e(x) = U_2$

Thus

$$N_1 = 1 \quad \text{at node 1}$$
$$N_1 = 0 \quad \text{at node 2}$$

Similar reasoning applies for N_2.

We can use the Kronecker delta, δ_{ij}, to represent N_i more concisely as:

$$N_i^e(x_j) = \delta_{ij} \begin{cases} 1 & i = j \\ 0 & i \neq j \end{cases} \tag{5}$$

It can be shown that N_1 and N_2 obey the following equations:

$$N_1 = \frac{x_2 - x}{\ell^e} \tag{6a}$$

$$N_2 = \frac{x - x_1}{\ell^e} \tag{6b}$$

where $\ell^e = x_2 - x_1$, the length of the element. The following observations can be made in regard to N_i:

1. $\sum_i N_i \equiv 1$, necessary

2. $$\sum \frac{\partial N_i}{\partial x} \equiv 0$$

The choice of shape functions, N_i, is not arbitrary. Certain convergence criteria have to be satisfied to ensure convergence to the desired result. In this regard, there are two minimum conditions that have to be satisfied to ensure convergence (monotonic); those are (1, 4, 6, 7, 22):

1. Interpolation functions should be such that interelement continuity of the functions are satisfied, and
2. The shape functions must be able to produce a constant strain condition, including zero strain (i.e., rigid body motion), through the element in the limit as the element size is reduced to infinitesimal dimensions. This means that the unknown function must be able to take a linear form throughout the element in the limit as the element size is decreased.

In the preceding example, a linear variation has been assumed, because through two points the curve that can be passed is a straight line. If we had three nodes per element instead, a parabola can be passed thus giving us a quadratic variation. For line elements, a family of polynomials (called Lagrangian polynomials) are easily formed and are used as shape functions. Those can easily be extended into two and three dimensions. The formula giving those polynomials is found in standard textbooks to be:

$$\ell_k(x) = \frac{\prod\limits_{\substack{i=1 \\ i \neq k}} (x - x_i)}{\prod\limits_{\substack{i=1 \\ i \neq k}} (x_k - x_i)} \quad \text{at node } k \tag{7}$$

At node k, the numerator and denominator are all equal and at any other node the numerator is zero, thus

$$\ell_k(x_i) = \delta_{ki} \qquad \text{is satisfied} \quad .$$

The accuracy of interpolation depends directly upon the order of completeness of the polynomial function assumed. This, in general, is directly related to the number of element nodes used for interpolation (21). Thus, the greater the number of degrees of freedom used, the more closely will our solution approximate the exact solution ensuring equilibrium, provided that in the limit the true variation of our variable can be approximated (22). Also, fewer elements can be used.

It is worthwhile noting that Lagrange polynomials used as interpolation functions provide us with the continuity of the variable U in our case, or C^0 continuity. There are other families, such as Hermite polynomials, that provide continuity of the variable and its derivatives at each node, or C^1, C^2, ... C^n continuity (7).

Strain-displacement relations. Those relations can be obtained from Strength of Materials or Elasticity textbooks.

For a truss element capable of axial elongation we have

$$\varepsilon_x = \frac{\partial u}{\partial x} \tag{8}$$

where u is displacement in x-direction.

For a plane stress condition:

$$\left\{ \varepsilon \right\} = \left\{ \begin{matrix} \varepsilon_x \\ \varepsilon_y \\ \gamma_{xy} \end{matrix} \right\} \tag{9}$$

where u = displacement in x direction

and v = displacement in y direction

In matrix form

$$\begin{bmatrix} \varepsilon_x \\ \varepsilon_y \\ \gamma_{xy} \end{bmatrix} = \begin{bmatrix} \frac{\partial u}{\partial x} \\ \frac{\partial v}{\partial y} \\ \frac{\partial v}{\partial x} + \frac{\partial u}{\partial y} \end{bmatrix} \tag{10}$$

<u>Stress-strain relations</u>. The stress-strain relations are also obtainable, for the problem considered, from elasticity references. They are special cases of the generalized Hookes Law:

For axial elements

$$\sigma = \varepsilon E \tag{11}$$

For plane stress

$$\begin{bmatrix} \sigma_x \\ \sigma_y \\ \tau_{xy} \end{bmatrix} = \frac{E}{1 - \nu^2} \begin{bmatrix} 1 & \nu & 0 \\ \nu & 1 & 0 \\ 0 & 0 & \frac{1-\nu}{2} \end{bmatrix} \tag{12}$$

Note: Equations (8) to (11) are valid for isotropic materials.

<u>Derive equilibrium equations</u>. In structural applications, nodal displacements corresponding to the equilibrium solution can be obtained by any of the following (1):

1. Principle of virtual work.
2. Weighted residuals technique. This method is basically a numerical technique. One assumes a trial function to represent an approximate solution.

The assumed function gives some error (residue). The resulting error is then minimized by some procedure such as the Least Squares method or the Galerkin method. This method is applicable to systems described by elliptic partial differential equations (1).

Principle of virtual displacements (direct approach). This procedure is analogous to the direct stiffness method in matrix structural analysis. This method deserves special attention. Most major general purpose programs have been written using the displacement based formulation, because of its simplicity, generality, and good numerical properties (2). To determine displacements corresponsing to the equilibrium solution we use the principle of minimum Total Potential Energy. It states, "Of all possible states of displacements, satisfying the geometric boundary conditions, the one that corresponds to the equilibrium state is the one that renders the total potential energy Π stationary (minimum)" (1). The potential energy Π consists of the strain energy U minus work done by external forces, W.

$$\Pi(\{u\}) = U - W \tag{13}$$

The equilibrium stiffness matrix [K] is obtained by minimizing Π with respect to nodal displacements $\{u\}$, that is

$$\frac{\partial \Pi}{\partial \{u\}} = \{0\} \tag{14}$$

For plane stress or plane strain, the stiffness matrix [K] is given by

$$[K] = \int_{\Omega} [B]^T [D] [B] \, d\Omega \tag{15}$$

where Ω is system domain

[D] is an elasticity matrix

and [B] is the strain matrix (6), which defines strains in terms of nodal displacements (4). Alternatively, the element stiffness matrix $[K^e]$ is given by a similar form

$$[K^e] = \int_{\Omega^e} [B^e]^T [D^e] [B^e] \, d\Omega^e \tag{16}$$

where the matrices $[K^e]$, $[B^e]$, and $[D^e]$ have the same meaning as [K], [B] and [D] of equation (15) with the superscript e indicating that they are for a single element e. Also, Ω^e is the domain of element e. [K] can also be given by the following:

$$[K] = \sum [K^e] \tag{17}$$

[B], for plane problems, is given by

$$[B] = \begin{bmatrix} \frac{\partial N}{\partial x} , & 0 \\ 0 , & \frac{\partial N}{\partial y} \\ \frac{\partial N}{\partial y} , & \frac{\partial N}{\partial x} \end{bmatrix}$$

where N is the matrix of shape functions. The equilibrium stiffness K ensures equilibrium in an overall sense only, and local violations on the element level exist but do not influence the solution results (1).

Assemble System Equation

After the stiffness matrix [K] is obtained, the system equations can be assembled. Those would be of the following form

$$[K]\ \{u\} = \{F\} \tag{19}$$

where [K] is system stiffness matrix

{u} is the displacements vector

{F} are the resultant forces

Load boundary conditions are reflected in {F}, that is known applied forces. We must also apply geometric boundary condtions in {u}, otherwise [K] will be singular. Upon applying geometric boundary conditons, we have eliminated any possible rigid body motions (1).

System Equation Solution

The system equation (Eqn. 19), is a system of linear algebraic equations relating nodal displacements {u}, and internal forces {F}, which are assumed to be concentrated at the individual element nodes. This procedure is a common one applicable to all matrix methods of structural analysis (21). The resulting algebraic equations involve a large number of unknowns which represent the various degrees of freedom of the elements.

The system stiffness matrix, [K], is the largest single matrix to be dealt with. It is a square matrix. If NDOF is the number of degrees of freedom of the system, the size of [K] is NDOF x NDOF, which can be very large. In most practical situations [K] is symmetric and banded about the diagonal. Assuming that [K] is symmetric and banded, as it is in most structural applications, the half bandwidth, IBW, becomes an important consideration, as shown in Figure 7 (1).

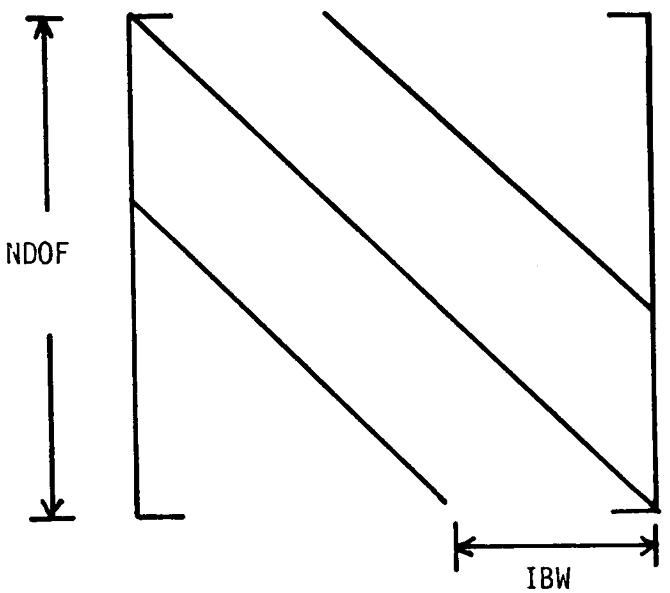

Figure 7. Banded Symmetric Matrix Showing Half Bandwidth, IBW.

The half bandwidth of a typical element, IBWE, is given by Equation 1.3, in reference 1, as

$$IBWE = NG \times (NDIFF + 1) \tag{20}$$

where NG = number of degrees of freedom per node

and NDIFF = maximum difference of node numbers of an element.

The system half bandwidth, IBW, is the maximum value of IBW, that is

$$IBW = IBWE_{MAX} \tag{21}$$

Thus node numbering is important when a banded solution is considered.

Another alternate approach is what is known as the frontal solution method. Hinton and Owen treat this method in detail in reference 6. Frontal solutions do not require the assembly of the overall system stiffness [K], because the equations are assembled and the variables simultaneously eliminated. This method is dependent on element numbering, and independent of node numbering.

Post Solution Calculations

After displacements are obtained, strains, stresses, and other quantities of interest (perhaps another loading condition) can be obtained by applying the proper relations.

IV. ISOPARAMETRIC ELEMENTS

So far, the interpolation functions dealt with have been used to describe the displacement field or, more generally, the field unknown variable. Also, the elements had simple linear boundaries. In the case of a curved boundary, it was approximated by straight lines.

In 1968, Ergatoudis et al. introduced a new type of elements called Isoparametric elements, which may have curved boundaries. The basic premise is that the same functions, N_i, used to define the displacement field are also used to define element geometry (6). For this purpose two coordinate systems will be used, a local coordinate system where model elements have simple shapes (straight boundaries), and a global system where the actual element takes on its general shape, which does not necessarily involve straight boundaries. For the purpose of presentation, consider a quadrilateral shaped element in two dimensions. Let x and y denote coordinates in the global system, and ξ and η be the coordinates in the local space. The element in global and local systems is shown in Figure 8 below.

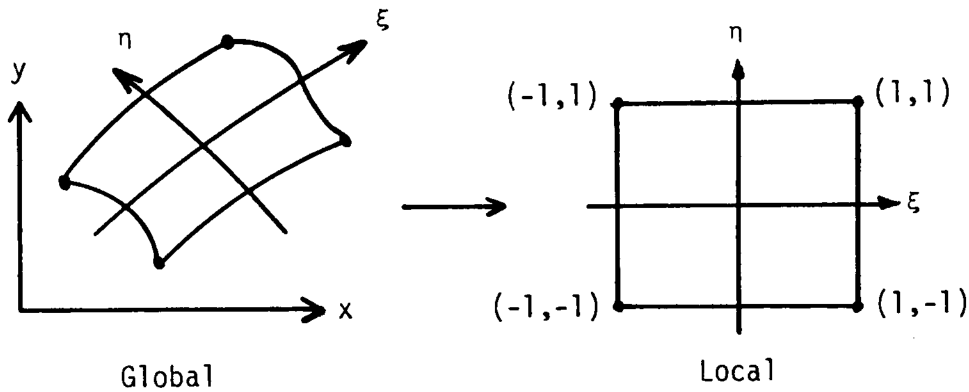

Figure 8. Isoparametric Element in Global and Local Systems.

Also note that local coordinates vary from $\xi = -1$ to $\xi = 1$ and from $\eta = -1$ to $\eta = 1$. This range of values is used because numerical integration is required, and because the range (-1, 1) is that used in conjunction with Gaussian quadratures (1).

As presented by Ergatoudis, et al. in their paper in 1968, in dealing with a displacement field with u and v as the displacement components of a node, it was stated that functions N_i describe displacements in the global space. Furthermore, it was assumed that the same N_i's can again be used in the local system. For displacements u and v we have:

$$u(\xi,\eta) = \Sigma N_i u_i = \{N\}^T\{u\} \tag{22a}$$

$$v(\xi,\eta) = \Sigma N_i v_i \quad \{N\}^T\{v\} \tag{22b}$$

(with $N_i = 1$ at node i and zero elsewhere).

Ergatoudis, et al. (4) prove that the convergence criteria stated before are automatically satisfied. Furthermore, displacement continuity between adjacent elements is satisfied with an equal number of nodes on each side and no internal nodes.

The stiffness matrix [K], for plane stress or plane strain, has been given by equation 15 as

$$[K] = \int_\Omega [B^T]\,[D]\,[B]\,d\Omega$$

where again Ω is solution domain, [D] is an elasticity matrix, and [B] is a strain matrix. It defines strains $\{\varepsilon\}$ in terms of nodal displacements $\{u\}$.

[B] is $$[B] = [B\ ,\ B\ ,\ .\ .\ .\ B] \tag{23}$$

where

$$[B_i] = \begin{bmatrix} \frac{\partial N_i}{\partial x} , & 0 \\ 0 , & \frac{\partial N_i}{y} \\ \frac{\partial N_i}{\partial y} , & \frac{\partial N_i}{\partial x} \end{bmatrix} \tag{24}$$

But the shape functions N_i have been defined in the local coordinate system. From the chain rule for partial derivatives we know that

$$\frac{\partial N_i}{\partial \xi} = \frac{\partial x}{\partial \xi}\frac{\partial N_i}{\partial x} + \frac{\partial y}{\partial \xi}\frac{\partial N_i}{\partial y}$$

and

$$\frac{\partial N_i}{\partial \eta} = \frac{\partial x}{\partial \eta}\frac{\partial N_i}{\partial x} \quad \frac{\partial y}{\partial \eta}\frac{\partial N_i}{\partial y}$$

Written in matrix form:

$$\begin{Bmatrix} \dfrac{\partial N_i}{\partial \xi} \\[2ex] \dfrac{\partial N_i}{\partial \eta} \end{Bmatrix} = \begin{bmatrix} \dfrac{\partial x}{\partial \xi} & \dfrac{\partial y}{\partial \xi} \\[2ex] \dfrac{\partial x}{\partial \eta} & \dfrac{\partial y}{\partial \eta} \end{bmatrix} \begin{Bmatrix} \dfrac{\partial N_i}{\partial x} \\[2ex] \dfrac{\partial N_i}{\partial y} \end{Bmatrix} = [J] \begin{Bmatrix} \dfrac{\partial N_i}{\partial x} \\[2ex] \dfrac{\partial N_i}{\partial y} \end{Bmatrix} \tag{25}$$

where [J] is the Jacobian matrix

Also, $\quad d\Omega = dx\ dy = |J|\ d\xi d\eta$

Now, integration can be carried out in the local system between the limits -1 and 1, thus

$$[K^e] = \int_{-1}^{1}\int_{-1}^{1} [B^{e^T}]\ [D^e]\ [B^e]\ |J|\ d\xi\ d\eta \tag{26}$$

where $[K^e]$ is the stiffness of an element. Often the integrand cannot be integrated simply, and numerical integration must be used.

A final remark is due on the use of isoparametric elements. For a given number of total nodal unknowns, NDOF, in a domain, better approximation is obtained with a smaller number of complex elements.

There is a theoretical error analysis substantiating this statement, if the solution obtained is sufficiently smooth. The order of the approximating polynomials, N_i, governed by the number of element nodes, determines the complexity of the element. Parabolic isoparametric elements (Figure 9) are in this context good performers, finding application in various types of analyses (6).

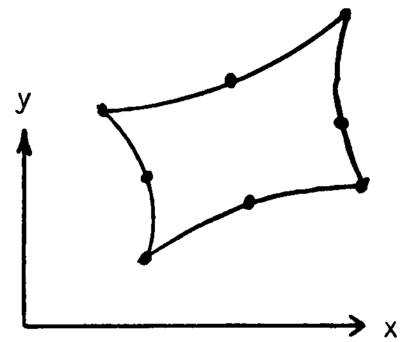

Figure 9. Parabolic Isoparametric Element in Global System.

V. CLOSURE

A final remark highlighting the differences between matrix analysis and finite element analysis is due.

As stated before, finite element analysis is applicable to many field or continuum problems. The solution obtained is, however, only approximate. In a general continuum problem, the region dealt with is at least two dimensional which necessitates the conformity of an area or volume element on all its boundaries. In matrix analysis, which is concerned mainly with skeletal structures, line elements (such as beam elements) are used and the boundaries on which displacement compatibility are the end sections, or joints. This fact renders line elements conformable, and "exact" solutions obtained (exact within the context of beam theory). Also stresses and stress resultants at any point, within a beam for example, can be uniquely determined by statics alone (12).

CHAPTER IV

FINITE ELEMENT MODEL

I. METHODS FOR OBTAINING M-ϕ CURVES

Moment-rotation (M-ϕ) curves for clip angle beam-column connections can be obtained by any of the following methods.

Derive Theoretical Equations

This approach to obtain M - ϕ curves was followed by Lothers (13). Equations for end moment M, and end rotation ϕ were obtained in terms of known angle properties and dimensions.

Experimental Methods

Numerous authors investigated Moment-Rotation characteristics of connections experimentally (9, 11, 16, 17, 19, 20). The most recent experiments were conducted at The University of Tennessee by Lennon (11). In his research, Lennon investigated M - ϕ characteristics of nine 4" x 4" angles. The thicknesses considered were 1/4". 3/8", and 1/2" respectively. Angle lengths were 6", 9", and 12" corresponding to 2, 3, and 4 bolts on each angle leg in the same order.

Finite Element Methods

Some researchers compared their experimental findings with the results of a finite element analysis (8, 17). The object of this work was to obtain M - ϕ curves of simple beam-column connections, investigated by Lennon, by a finite element approach. Those curves were compared with Lennon's curves for the same connections. The simple beam-column connections that were investigated are shown in Figure 10. Those are from Lennon's Figure 5 (11).

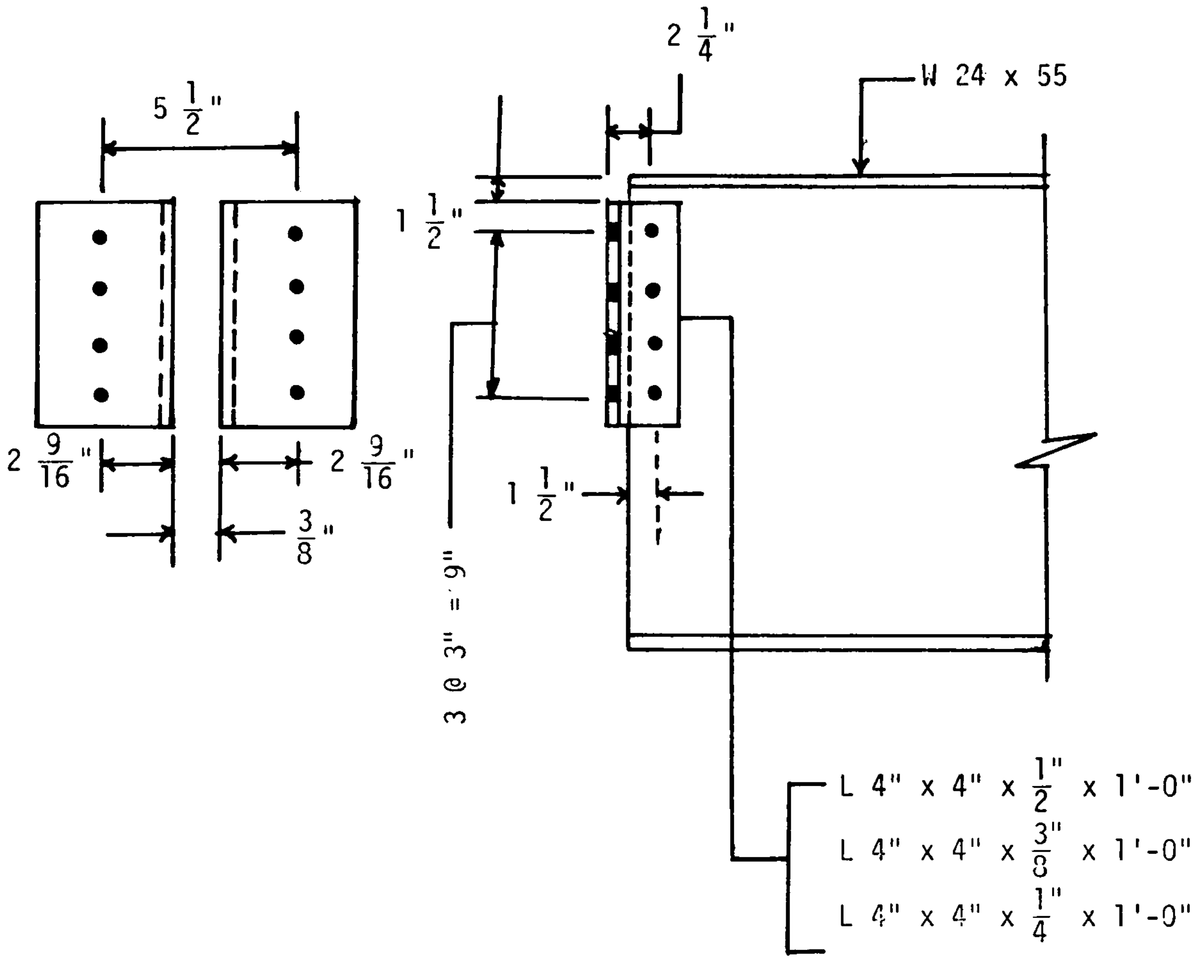

Figure 10. Beam to Column Connections Investigated.

II. COMPUTER PROGRAM USED

The computer code used in all analyses was PAFEC (Programs for Automatic Finite Element Calculations). PAFEC has mesh generation facilities, non-linear material capabilities, as well as plotting facilities. Mesh generation capabilities minimizes geometric input data. data. PAFEC solves system equations by the Frontal Method. This feature is especially helpful in iterative schemes, such as inelastic solutions. Most PAFEC elements are isoparametric (18).

Three types of elements were used (18). Those were:

1. PAFEC element 36210. This is an eight noded plane stress isoparametric element.
2. PAFEC element 36240. This is a six noded plane stress isoparametric element.
3. PAFEC element 30100: This is a two node spring element.

III. ASSUMPTIONS USED TO OBTAIN FINITE ELEMENT MODEL

The problem was idealized as a two-dimensional plane stress problem. This idealization was used by previous investigators (8, 17). The steel was idealized as an elastic-perfectly plastic (no strain hardening) material (see Figure 11). Yield stresses obtained by Lennon were used (11).

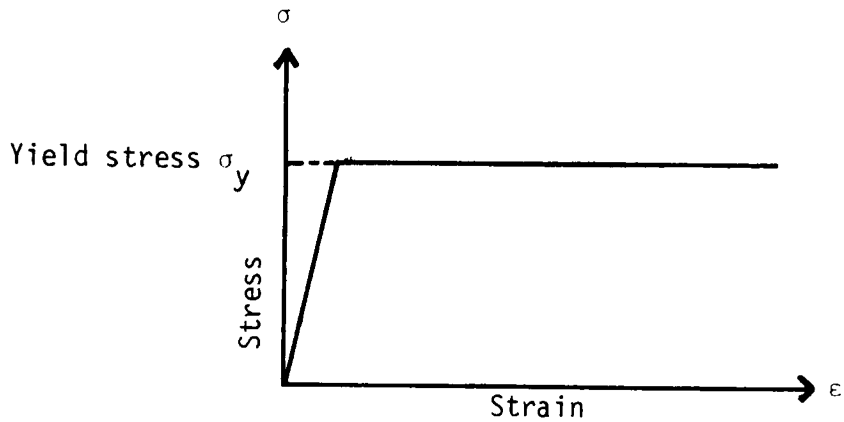

Figure 11. Idealized Stress-Strain Curve for Steel.

Beam Model

A W24 x 55 wide flanged beam was used in all investigations. Its dimensions were obtained from the A.I.S.C. Steel Construction Manual, 7th edition.

Two types of plane stress isoparametric elements were used in the beam. Those were the following.

1. Eight noded elements (3 nodes per side) were used for the web.
2. Six noded elements (3 nodes on two opposite sides) were used for the flanges.

Each node has two displacement degrees of freedom $u(u_x)$ and $v(u_y)$ as is shown in Figure 12.

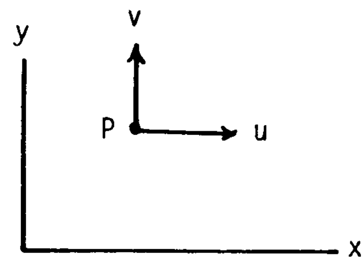

Figure 12. Nodal Degrees of Freedom for a Typical Node P.

Interelement compatibility was provided by having the same number of nodes on element boundaries. Web-flange element continuity is shown in Figure 13.

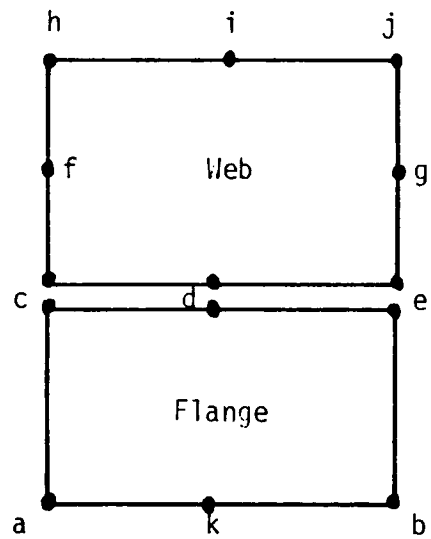

Figure 13. Web-Flange Interfacing Elements. (a) Linear Variation of Displacements along Edges ac and be; (b) Quadratic Variation of Displacements along Other Edges.

The load was applied at 6-3/4" from the free end of the beam in the experiment. In the model, only that portion of the beam between the load and the connection was included. This simplification has little (or no) effect on the column end displacements of the beam. Were the effect of the load on the stresses at the point of application of the load of primary importance, the entire beam would have been included in the model (see Figure 14).

Angle and Column Bolts Models

Angle. Three angles were investigated. Those were:

1. 4" x 4" x 1/4" x 1'-0"
2. 4" x 4" x 3/8" x 1'-0"
3. 4" x 4" x 1/2" x 1'-0"

Eight noded plane stress elements were used in the angle mesh. Angle elements had two thicknesses. The element thickness for the leg connected to the beam was varied in each run. This thickness was the actual angle thickness. The bolt line connecting the angle leg to the column was assumed to be completely fixed (see Figure 15). The shaded portion of Figure 15(b) was considered to have little or no contribution to the stiffness of that leg. Thus the effective width was considered to be 2-1/4", the distance from the centerline (℄) of column bolts to the edge of the angle.

Column Bolts. The bolts connecting column and angle together were out of the plane of the web. They were modeled as spring elements. If their simple spring stiffness, $K = \frac{AE}{L}$, was used this would have been equivalent to having them in the plane of the web. Furthermore, the

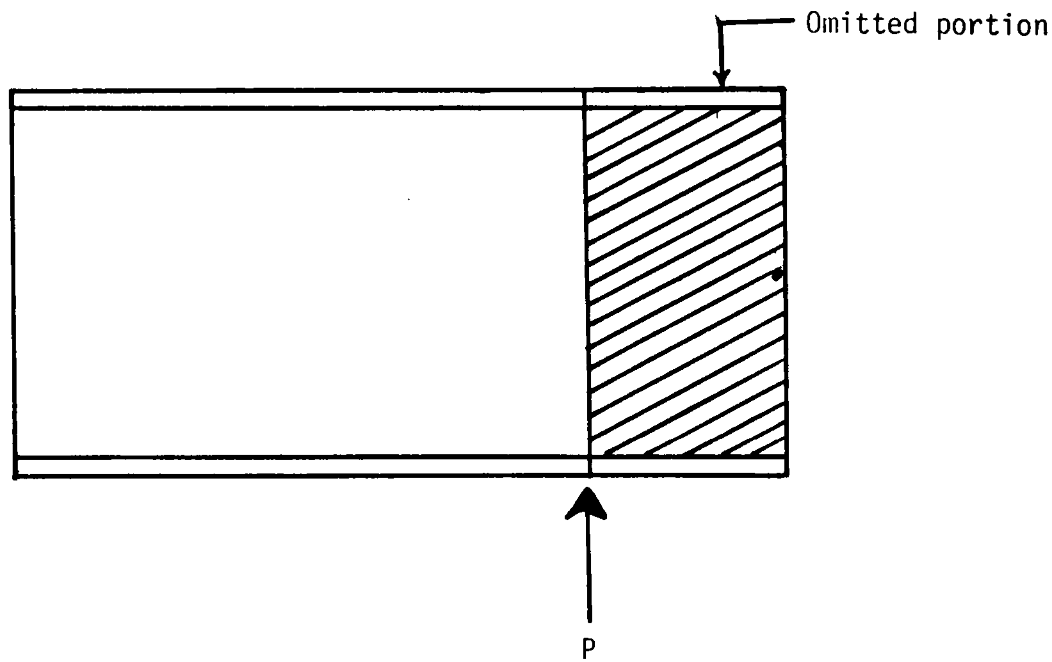

Figure 14. Beam Portion Omitted from Analysis Shown Striped (Figure Not to Scale).

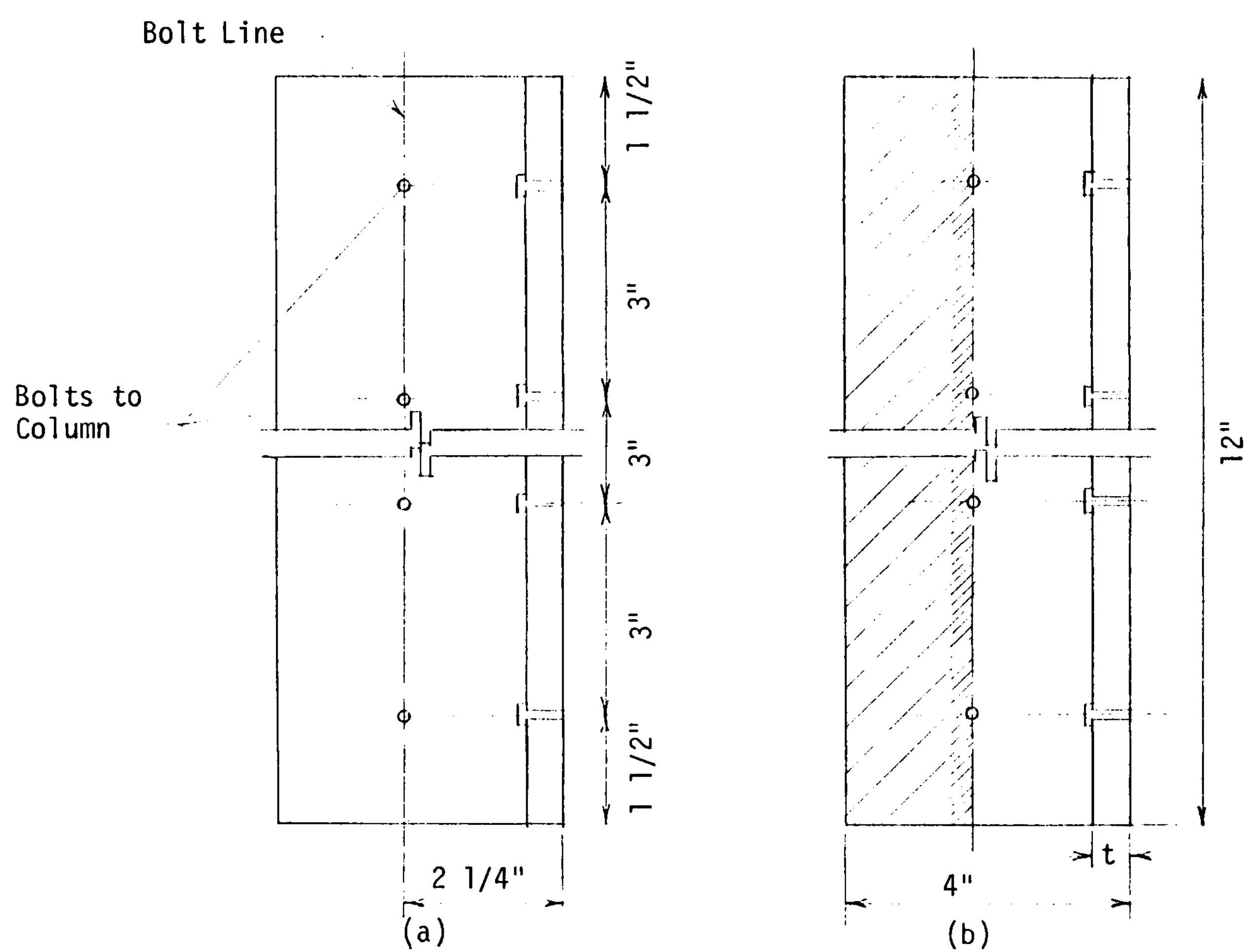

Figure 15. (a) Angle Showing Front View of Angle. Plate Connecting to Column Together with Column Bolts and Their Bolt Line; (b) Bolt Line was Considered Fixed, and Angle Plate Portion to Its Left was Omitted (Shown Striped) in Calculating Equivalent Bolt Stiffness.

simple spring stiffness would have overestimated their stiffness contribution to the actual physical system. The following method (Figure 16) was considered to obtain the equivalent bolt and angle stiffness.

Figure 16(a) shows the original undisplaced shape of the portion of the angle between the two bolt lines. This method considers the total displacement Δ of the joint from the column face to be made up of two displacements d_p and d_b as shown in Figure 16(b). Displacement d_p is the plate movement of joint B, while d_b is the displacement of angle away from column face due to bolt extension. The four bolts are assumed to extend equally by the amount d_b. The displacement d_p induces in AB moments and shears as shown in Figure 16(c).

From Figure 16(b) we have

$$\Delta = d_p + d_b \qquad \text{(i)}$$

$F_b = k_b \times d_b$, where

$K_b = \frac{AE}{L}$, axial stiffness of bolt

but total shear is $4 \times F_b$, therefore

$$P = 4F_b = 4K_b\, d_b$$

$$\therefore\ d_b = \frac{P}{4K_b} = \frac{PL}{4AE} \qquad \text{(ii)}$$

also $P = \frac{12EI}{L^3}\, d_p$, therefore

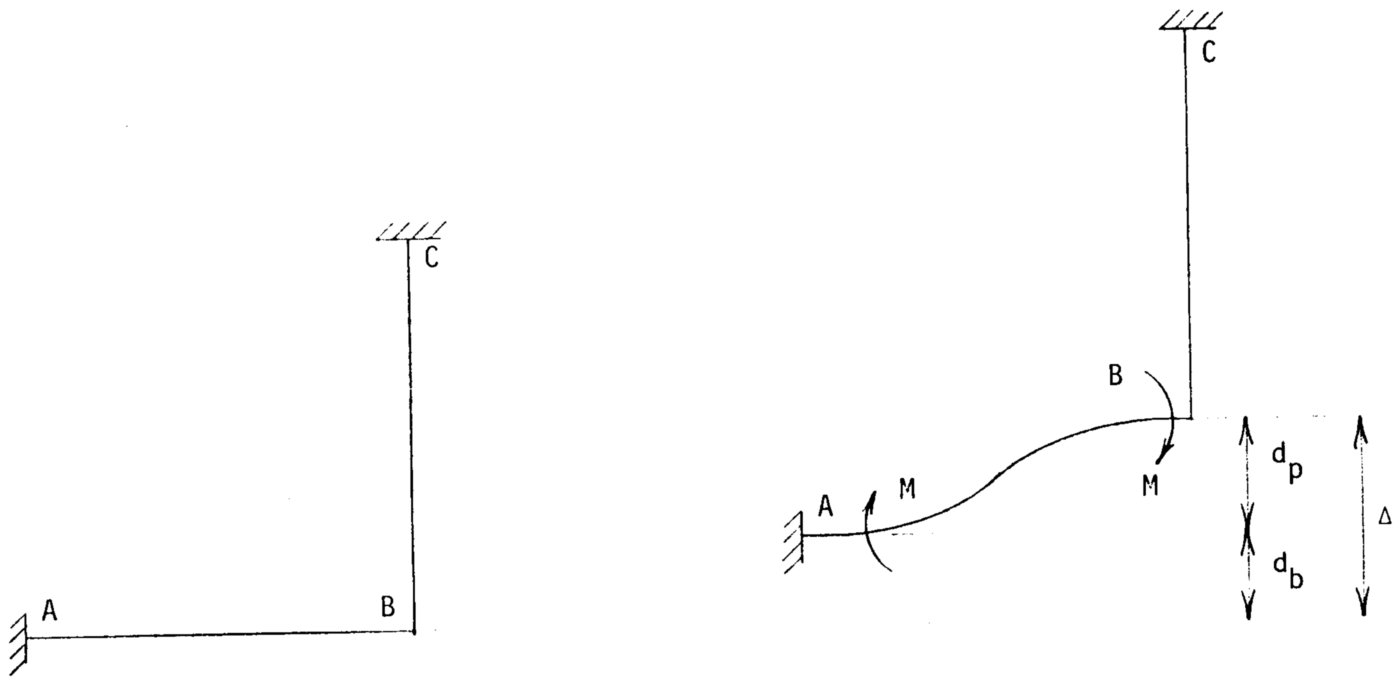

(a) Original Geometry

(b) Displaced Geometry

Figure 16. Derivation of Equivalent Bolt and Angle Stiffness Showing (a) Original Geometry; (b) Displaced Geometry; (c) Final Shears and Moments on AB.

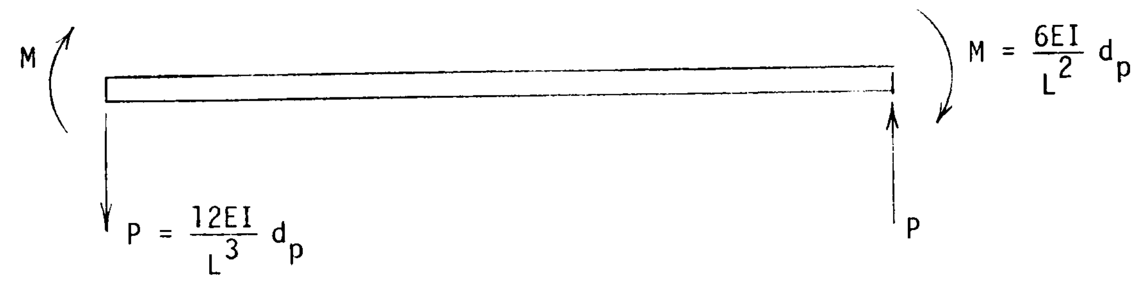

(c) Final Shears and Moments on AB

Figure 16 (continued)

$$d_p = \frac{PL^3}{12EI} \qquad \text{(iii)}$$

but $P = 4 \times \Delta \times K_{eg}$, where K_{eg} is the equivalent spring stiffness. This gives

$$\Delta = \frac{P}{4 \times K_{eg}} . \qquad \text{(iv)}$$

Substituting Eqs. ii, iii, and iv into Eq. i gives

$$\frac{P}{4K_{eg}} = \frac{PL^3}{12EI} + \frac{PL}{4AE} . \qquad \text{(v)}$$

When v is reduced we obtain the following final equation:

$$\frac{1}{K_{eg}} = \frac{L}{AE} + \frac{L^3}{3EI} . \qquad (27)$$

Boundary Conditions

Angle-column boundary conditions. Two models for angle-column boundary conditions were tried.

1. With a fixed center of rotation

The center of rotation is a point about which relative displacement of points (nodes) occurs. The centers of rotation of the angles varied and were determined by Lennon to be located at approximately 2-1/2" below the top flange (11). This position was coincident with the center-line of the topmost bolt connecting the angle to the column. The node corresponding to that location was restrained from movement ($u = v = 0$) (see Figure 17(a)). This condition was tried for the 1/2" angle, and was not used in the final model.

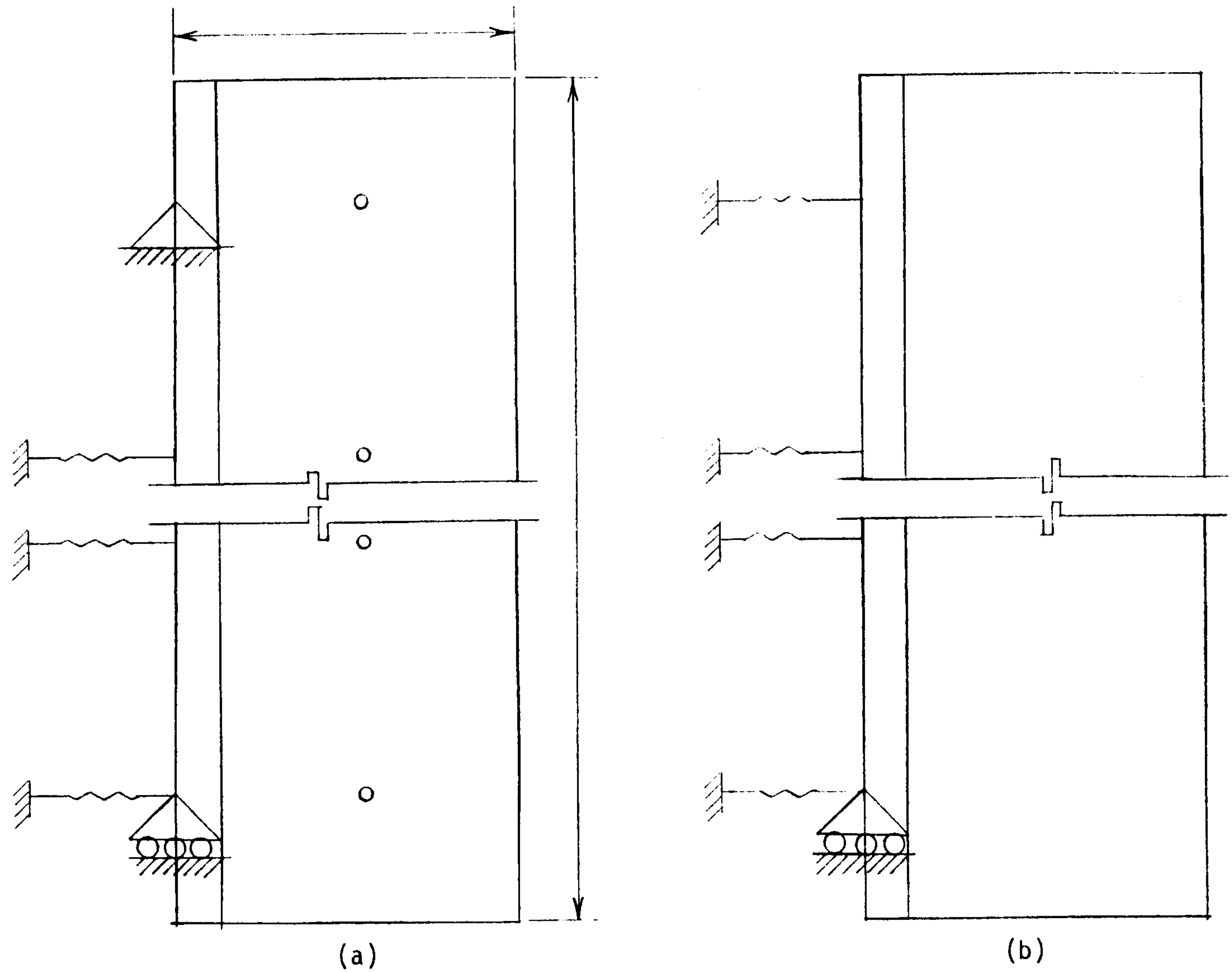

Figure 17. Idealization of Bolts as Springs and (a) Boundary Conditions Showing Fixed Center of Rotation; (b) Boundary Conditions Showing Variable Center of Rotation.

2. With a variable center of rotation.

To allow for a variable center of rotation, column bolts were treated as springs, with the lowermost angle spring node treated as a roller support ($v = 0$). This model was used in all cases considered (see Figure 17(b)). As a check the uppermost angle spring node was treated as a roller, and the same results were obtained.

Angle-web boundary conditions. Bolts connecting the angle and the beam web were represented by eight nodes, four nodes on the geometry describing the geometry of both the angle and the beam (see Figure 18). To assure that the eight nodes describe the four bolts only, the x-coordinate of the four nodes in the angle was offset by 0.01". Since each corresponding pair of nodes had identical degrees of freedom, the web nodes and the offset angle nodes tied together to simulate this condition by using the REPEATED.FREEDOMS module in PAFEC.

Owing to geometric and loading symmetry, half symmetry was used to reduce dimensions and loads (see Figure 19). The x-y plane has $u_z = 0$. This condition was invoked by setting $u_z = \theta_x = \theta_y = \theta_z = 0$, because with spring elements 6 degrees of freedom per node are assigned automatically.

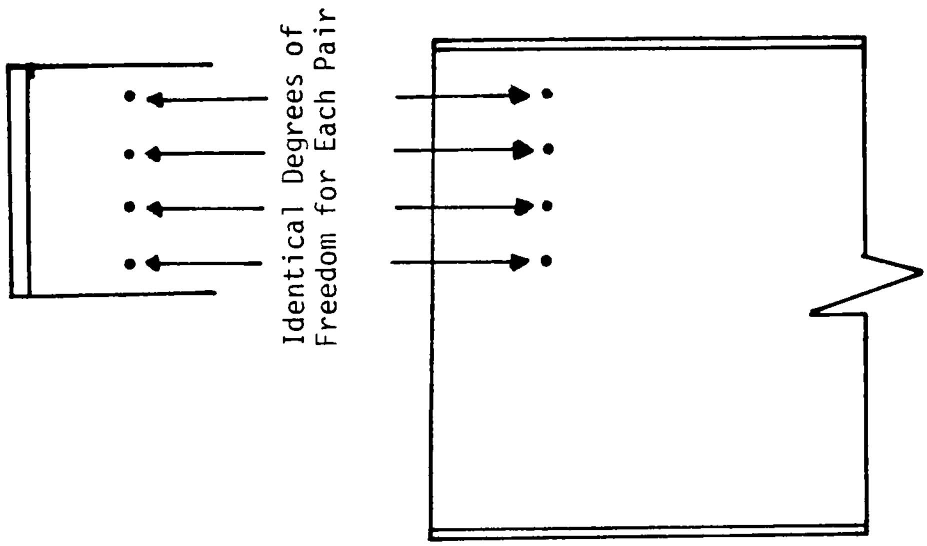

Figure 18. Web-Bolt Idealization Showing Identical Freedoms Used.

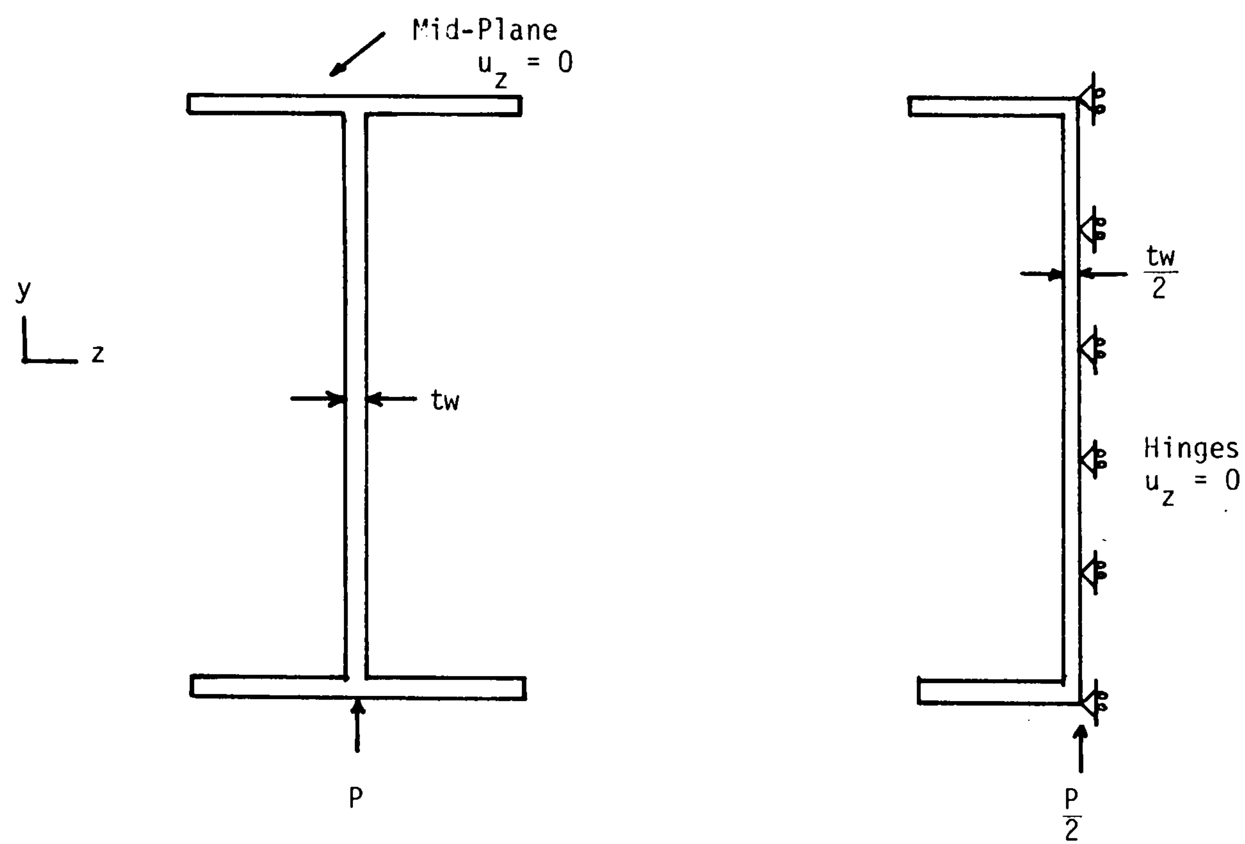

Figure 19. Half-Symmetry Considerations for Beam X-Section.

CHAPTER V

RESULTS AND DISCUSSION

I. GENERAL

The same finite element mesh was used in all cases considered. The mesh is shown in Figure 20.

Computer output was divided into five groups of output. Those were:

1. Reactions at constraints and prescribed displacements.
2. Nodal displacements, u and v, for all nodes in the structure.
3. Plots of the displaced shape of structure and graphs showing variations of displacements along selected lines of nodes in the structure.
4. Spring end forces.
5. The two principal stresses σ_1 and σ_2, as well as the maximum shearing stress τ_{12}, for nodes in the angle.

The following values were obtained from the program output.

$U_{x,3}$, $U_{x,7}$, $R_{y,2}$, $\sigma_{1,29}$, $\sigma_{2,29}$, $\tau_{12,29}$

where

U_x denotes horizontal displacements in inches (in),

R_y denotes equivalent vertical reactions in pounds (lbs),

σ_1 denotes maximum principal stress in pounds per square inch (psi),

σ_2 denotes minimum principal stress in pounds per square inch (psi),

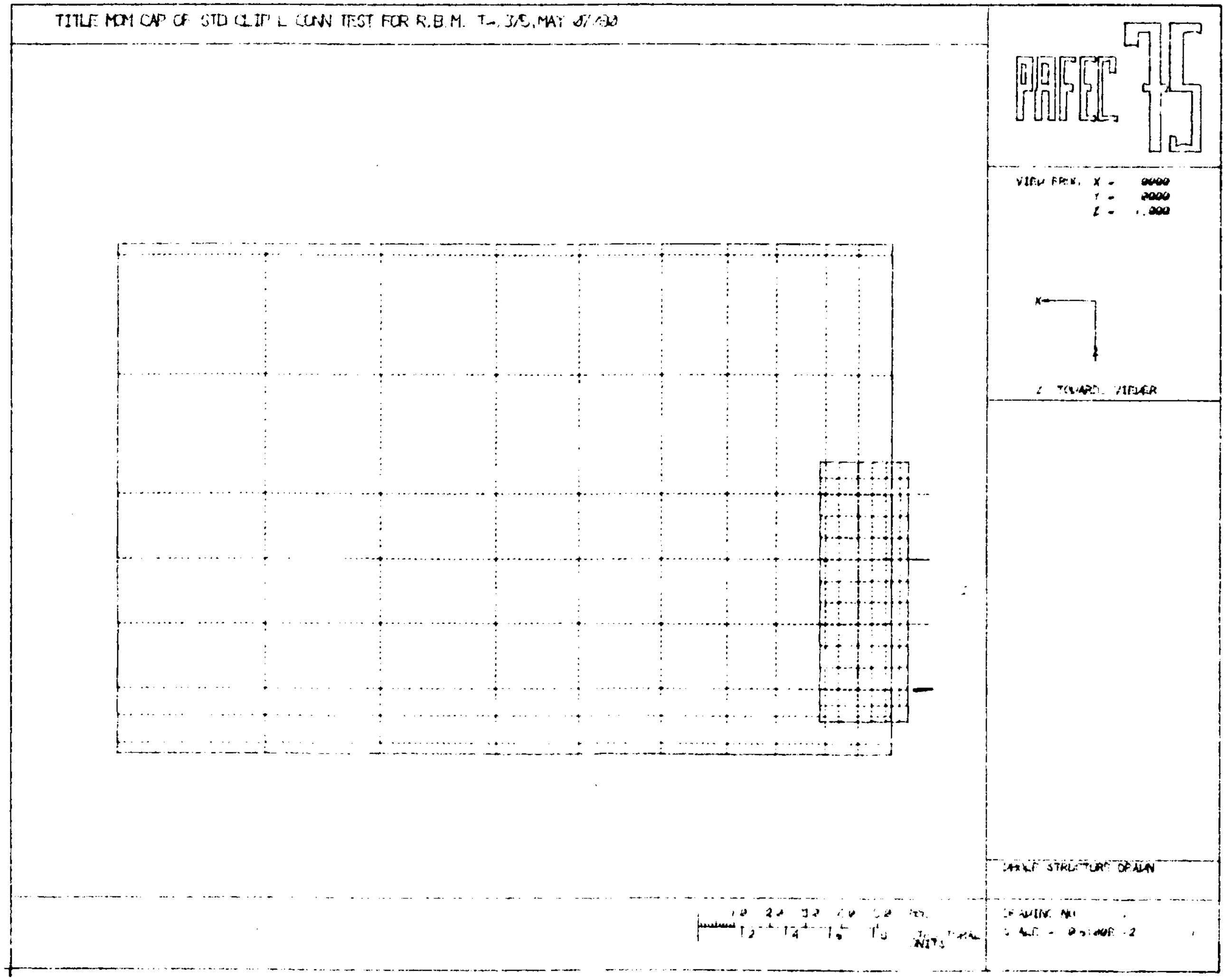

Figure 20. Computer Plot of Finite Element Mesh.

τ_{12} denotes maximum in-plane shear stress,

and the numbers appearing after the comma in subscripts give the node number at which that quantity was read.

The end rotation, ϕ, was calculated using Eq. 2, page 14, where Δ denotes the displacement of node 7 with respect to that of node 3, both lying on the beam end closer to the column face (see Figure 21). These nodes correspond to the positions of the dial gauges in the experiment (11).

The center of rotation at y inches measured from the beam top was determined by the following equation:

$$y = h \cdot \frac{u_7}{u_3 + u_7} . \tag{28}$$

Since the material was assumed to behave elastically, y remained unchanged.

In all cases, a displacement was applied at node 2 (Figure 21), as the load case, because such a load boundary condition usually results in better numerical conditioning for the solution. The computer results gave the equivalent nodal force that would have been applied to give such a displacement. Node 2 corresponded to the point of load application in Lennon's experiments. With the equivalent nodal force so computed, the moment M at the face of the column was obtained. Since the output gave the two principal stresses, σ_1 and σ_2, and the maximum in-plane shearing stress, τ_{12}, it was decided to calculate the effective stress, σ_{eff}, as given by Eq. 29(b) as a measure of the extent of stress at a point (node), in order that it be compared to the yield point stress for extrapolation. The effective stress, σ_{eff}, used for comparison was taken as

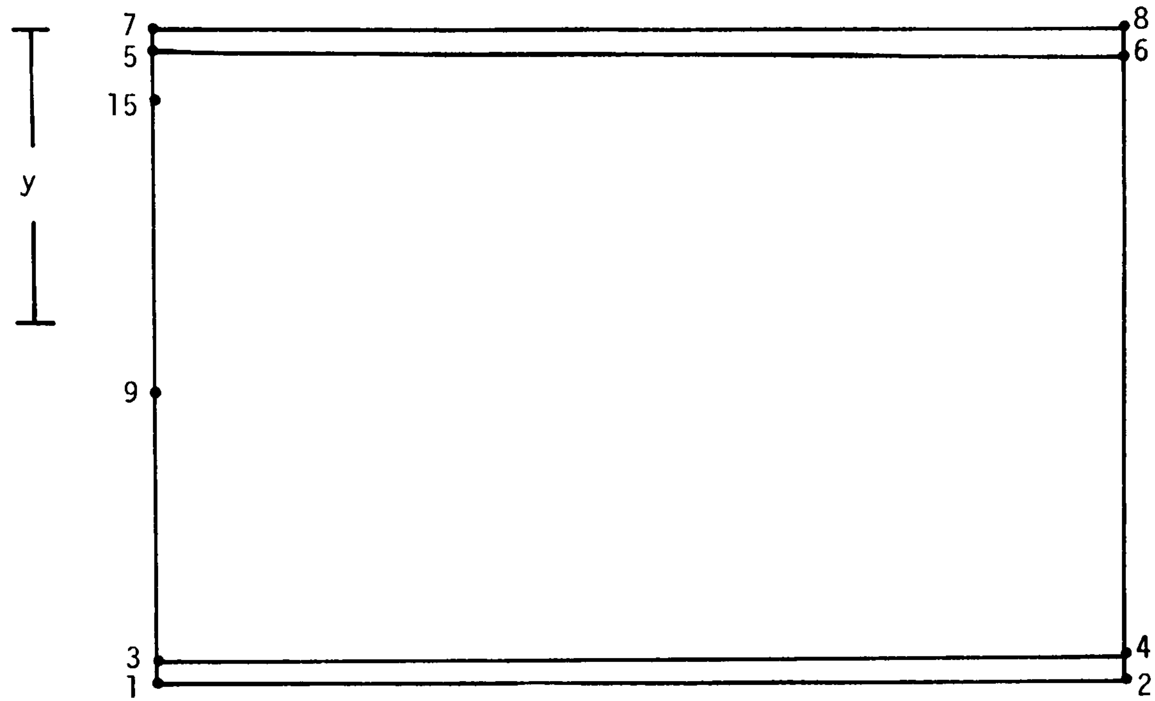

Figure 21. Beam Nodes Used for Calculations.

$$\sigma_{eff} = \frac{1}{\sqrt{2}} [(\sigma_1-\sigma_2)^2 + (\sigma_2-\sigma_3)^2 + (\sigma_3-\sigma_1)^2 + 6(\tau_{12}^2 + \tau_{23}^2 + \tau_{31}^2)]^{1/2}. \tag{29a}$$

In plane stress problems $\sigma_3 = \tau_{23} = \tau_{31} = 0$, thus

$$\sigma_{eff} = \frac{1}{\sqrt{2}} [(\sigma_1-\sigma_2)^2 + \sigma_2^2 + \sigma_1^2 + 6\tau_{12}^2]^{1/2} . \tag{29b}$$

The last equation was used to obtain the effective stresses, as a measure of the state of stress at a node. It was observed that the node corresponding to the lowermost angle-web bolt was the highest stressed, from the value of σ_1. This agreed with the physical reasoning that the lowest bolt took the larger share of the load.

The moment and rotation so obtained were linearly extrapolated to obtain the yield point moment, M_y, and the corresponding rotation at yield, ϕ_y. This was justified by the validity of linear elastic behavior of steel. The uniaxial yield point stress, σ_{yp}, was measured experimentally by Lennon (11).

II. RESULTS AND CALCULATIONS

Sample calculations for t = 0.25"

$U_{x,3} = 1.974 \times 10^{-2}$ in

$U_{x,7} = -0.948 \times 10^{-2}$ in

$R_{y,2} =$ 207 lbs

$\sigma_{1,29} =$ 5120 psi

$\sigma_{2,29} =$ -11 psi

$\tau_{12,29} =$ 2565 psi

$$= \frac{U_3 - U_7}{h} = \frac{U_3 - U_7}{23}$$

$$\phi = \frac{1.9744 + 0.9479}{2300} = 12.7 \times 10^{-4} \text{ rad.}$$

$$M = F_{y2} \times d$$

$F_{y2} = 2R_{y2}$ from half symmetry

$$M = 2 \times R_{y2} \times 3 = 124 \text{ lb-ft}$$

$$= 1.24 \text{ kip-ft}$$

$$\sigma_{eff} = \frac{1}{\sqrt{2}} \sqrt{(5131)^2 + (5120)^2 + (11)^2 + 6(2565)^2}$$

$$= 6783 \text{ psi}$$

Extrapolating to yield

$$\sigma_y = 42800 \text{ psi}$$

$$\therefore \phi_y = 12.7 \times 10^{-4} \times \frac{42800}{6783} = 80.1 \times 10^{-4} \text{ rads.}$$

and $M_y = 1.24 \times \frac{42800}{6783} = 7.82$ kip-ft.

Results for the remaining two thicknesses were obtained similarly and are summarized in Table 1.

TABLE 1

SUMMARY OF RESULTS

t ins.	$U_{x,3}$ x 100 ins.	$U_{x,7}$ x 100 ins.	$R_{y,2}$ lbs	$\sigma_{1,29}$ psi	$\sigma_{2,29}$ psi	$\tau_{12,29}$ psi	ϕ x 10^4 rads	M kip-ft	σ_{eff} psi	ϕ_y x 10^4 rads	M_y kip-ft
0.25	1.974	-0.948	207	5120	-11	2565	12.7	1.24	6783	80.1	7.82
0.375	0.981	-0.463	319	5400	24	2700	6.28	1.91	7135	37	11.24
0.5	1.492	-0.687	947	12310	139	6156	9.48	5.68	16234	23.35	14.00

The locations of the center of rotation, measured from the tension end of the clip angle, were found to be at 6.04", at 6.12", and at 6.24" for the 1/4", the 3/8", and the 1/2" thicknesses, respectively. Those locations remained unchanged for various loads due to the assumption of linear elastic behavior of the steel.

Figures 22-30 are computer plots, three for each angle thickness and in the order of increasing angle thickness. These are plots of:

1. The displaced structure, shown dotted, superimposed on the original undisplaced shape.
2. (a) Variation of horizontal displacement (U_x) for nodes along the beam end, and

   (b) Variation of horizontal displacement (U_x) of all nodes along the line joining the web bolts in the angle.
3. (a) Variation of vertical displacemtnt (U_y) of nodes lying along the lower end of the beam, as well as

   (b) Variation of horizontal displacement (U_x) of nodes along the web end just underneath the angle.

Results obtained for yielding, from the finite element analysis, were compared with the observed experimental results and the theoretical results by applying Lothers' equations, as obtained by Lennon (11). These results are listed below in Table 2 and illustrated graphically in Figures 31-33.

III. DISCUSSION OF RESULTS

From the results listed in Table 2 and illustrated graphically in Figures 31-33, the following observations were made.

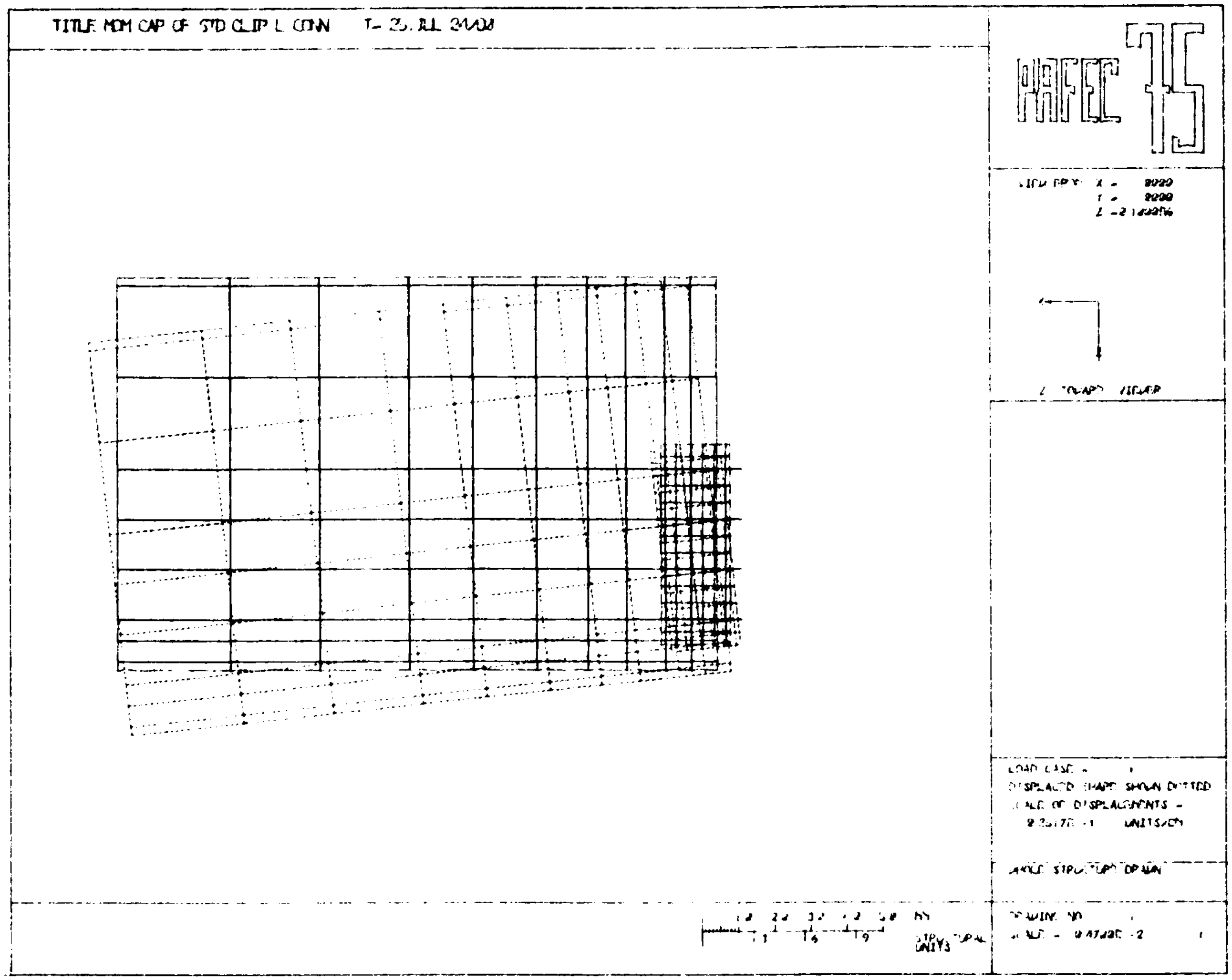

Figure 22. Displaced Shape for t = 0.25".

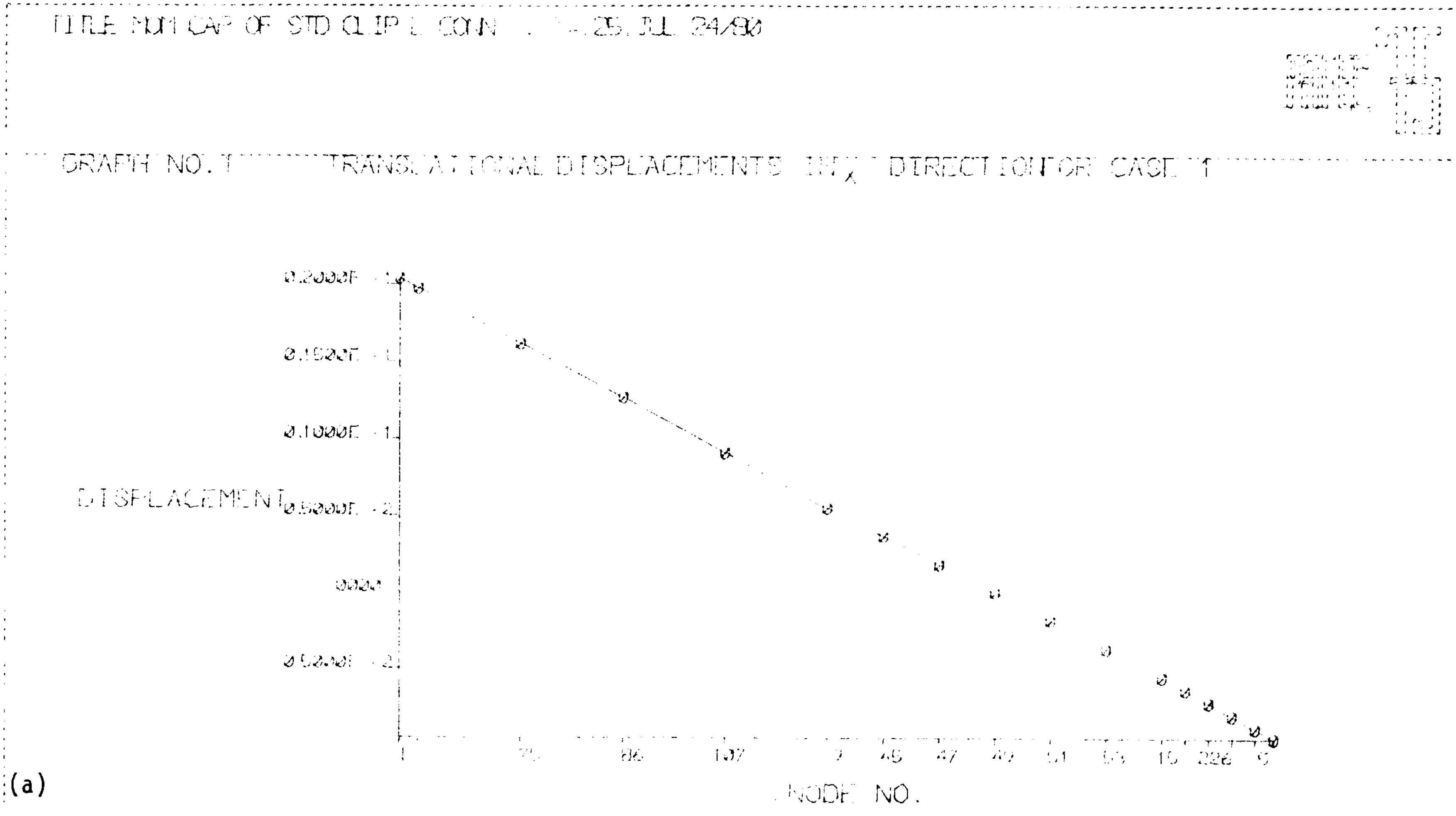

Figure 23. (a) Variation of U_x along Beam End for t = 0.25"; (b) Variation of U_x along Line Joining Web Bolts for t = 0.25".

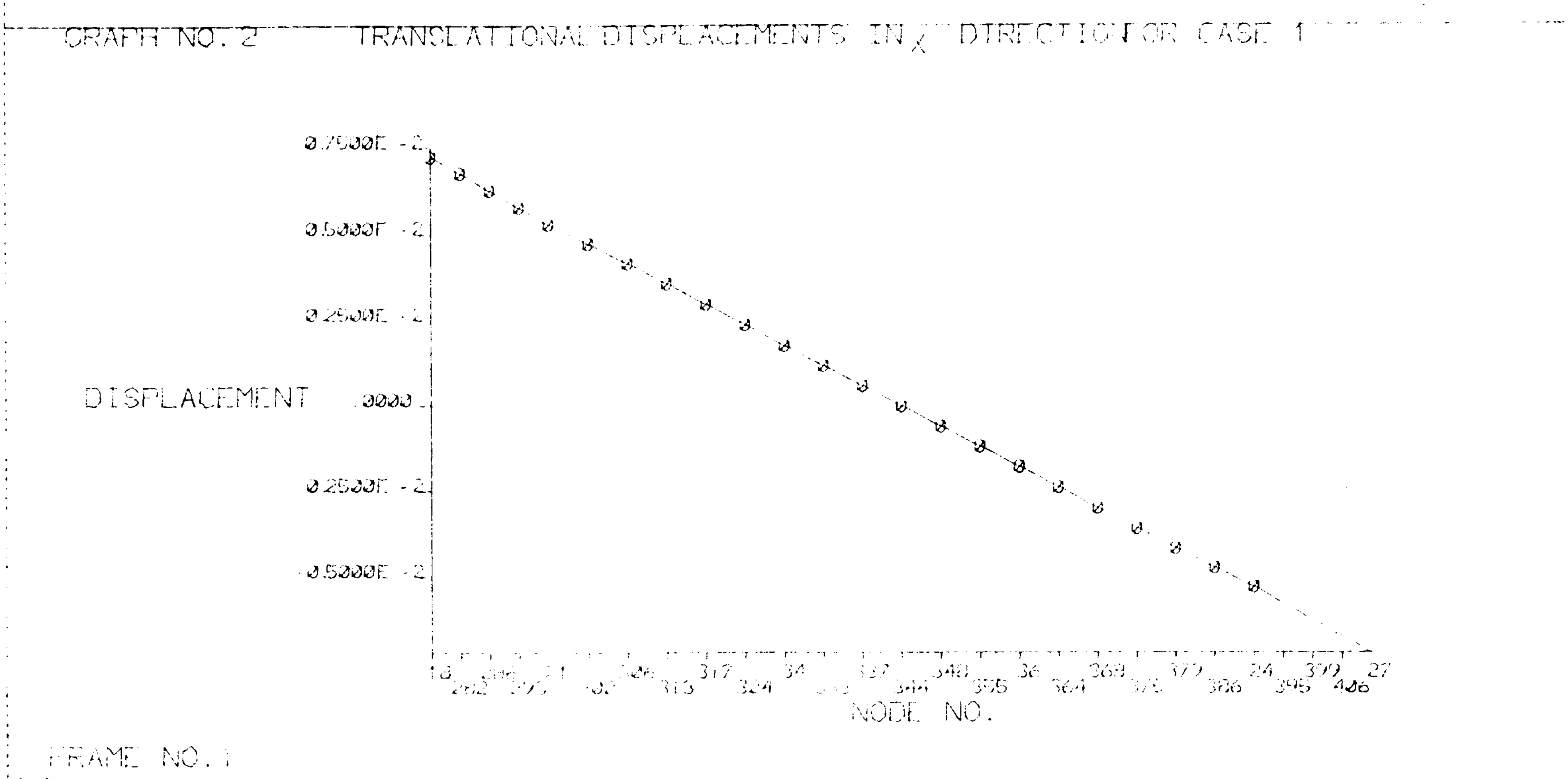

(b)

Figure 23 (continued)

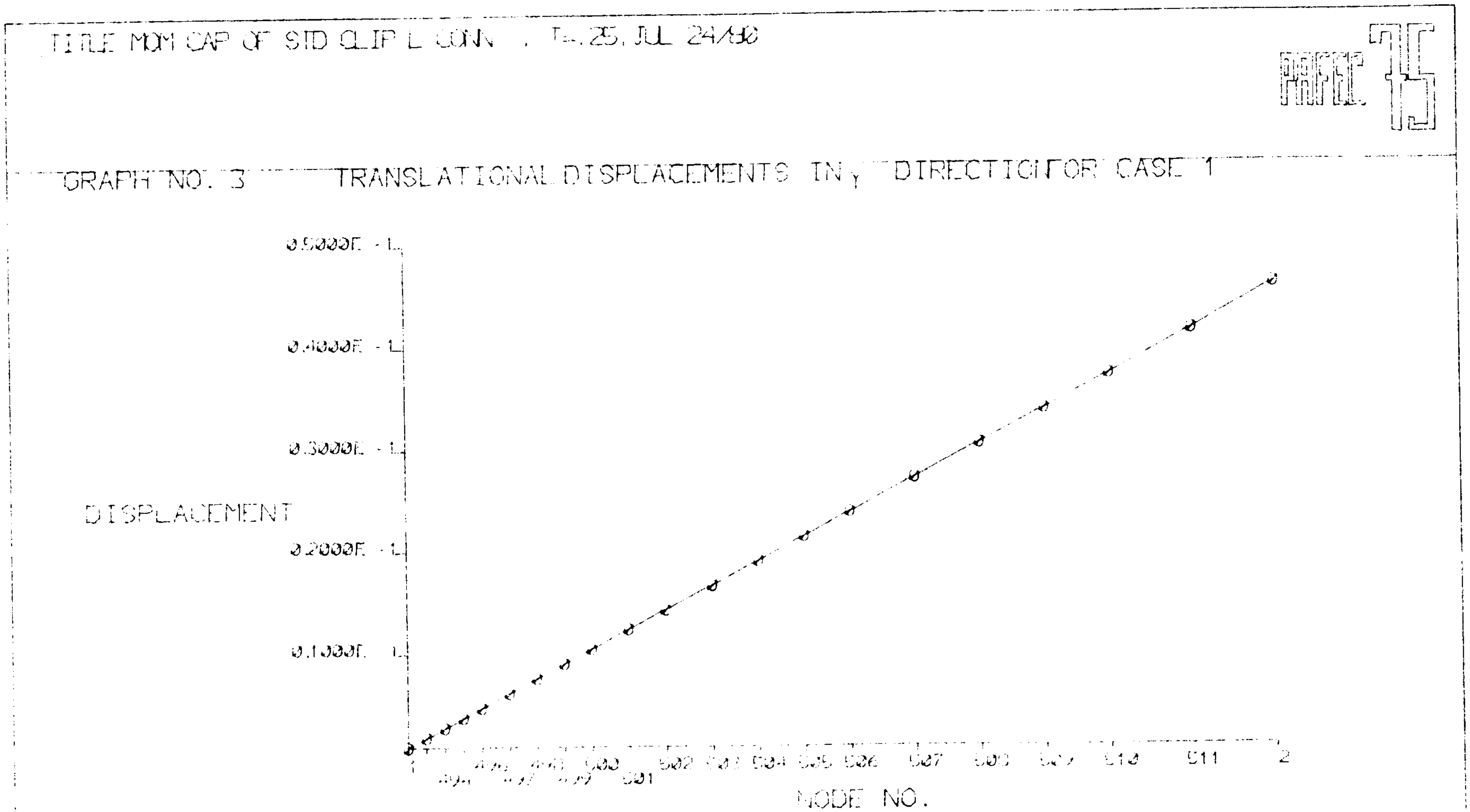

(a)

Figure 24. (a) Variation of U_y along Beam Bottom for t = 0.250"; (b) Variation of U_x along Beam End Just Beneath Angle for t = 0.250".

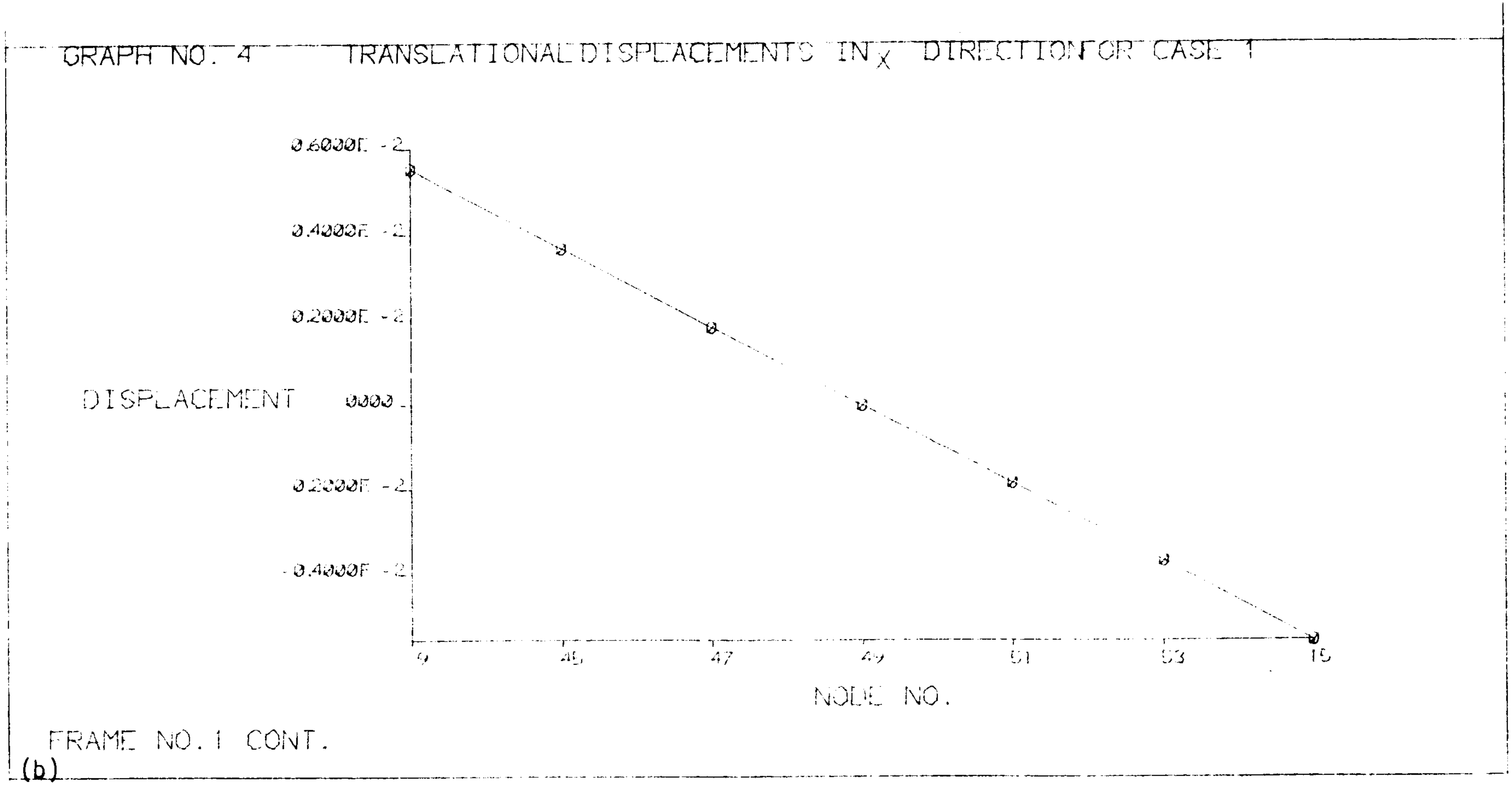

Figure 24 (continued)

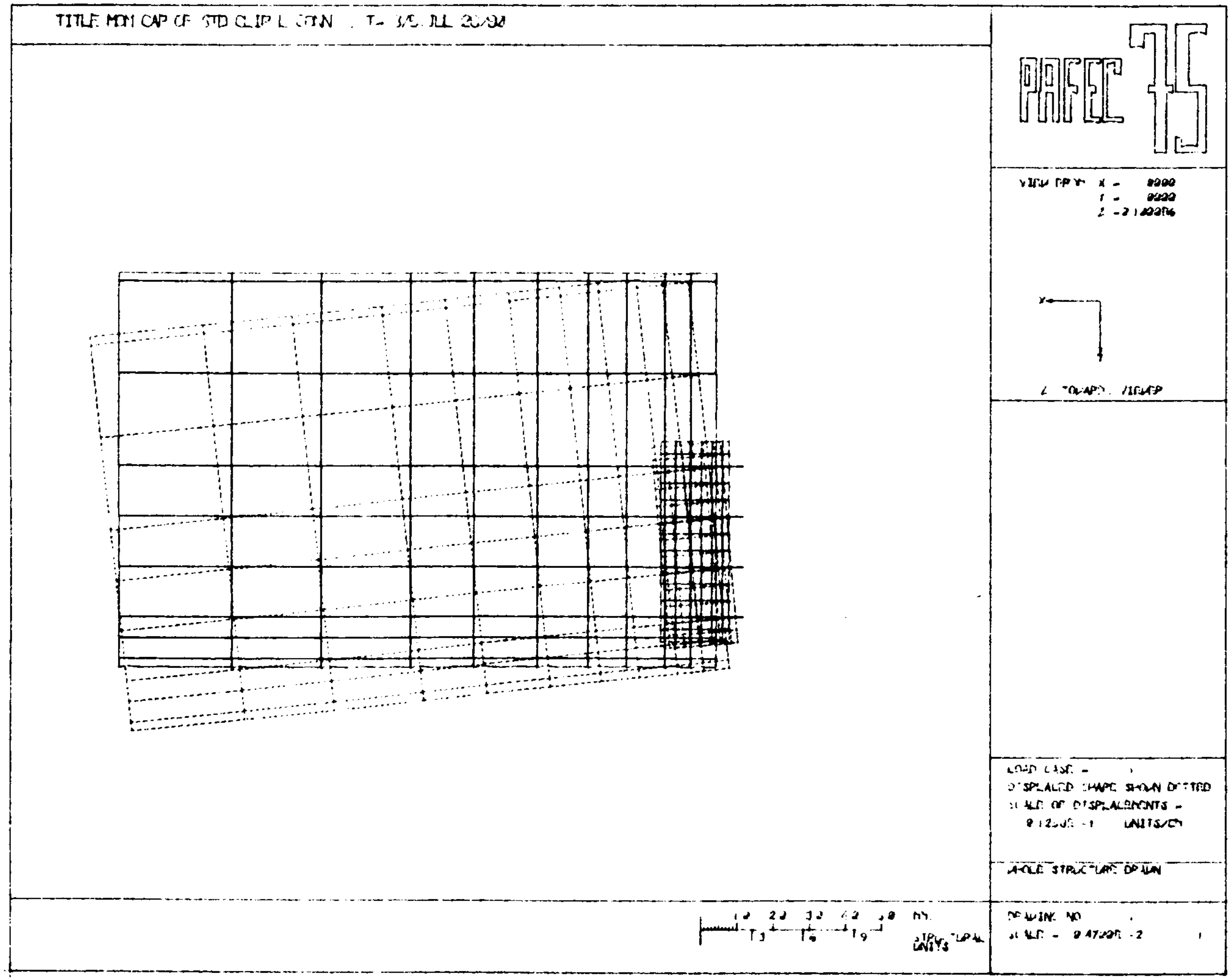

Figure 25. Displaced Shape for t = 0.375".

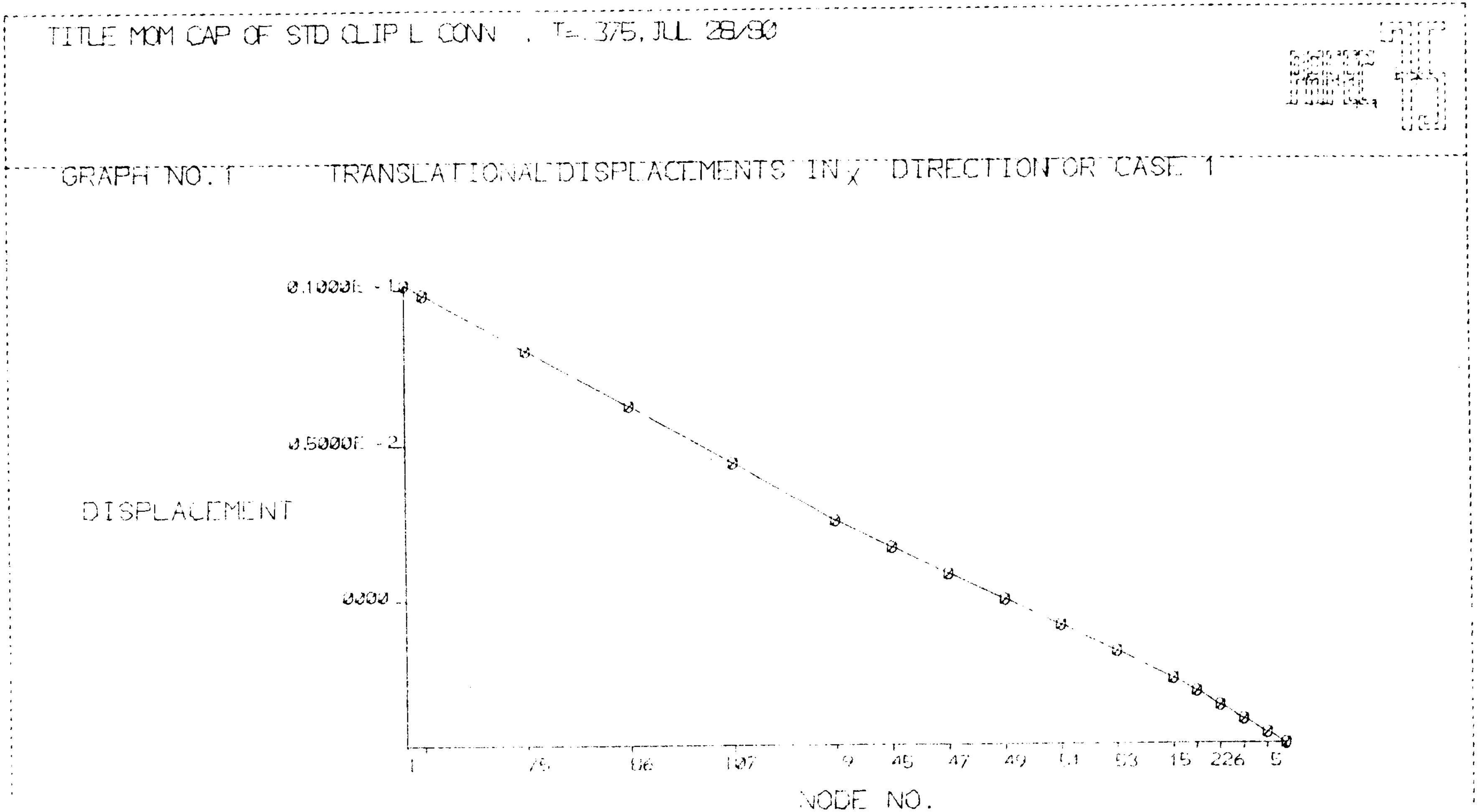

(a)

Figure 26. (a) Variation of U_x along Beam End for t = 0.375"; (b) Variation of U_x along Line Joining Web Bolts for t = 0.375".

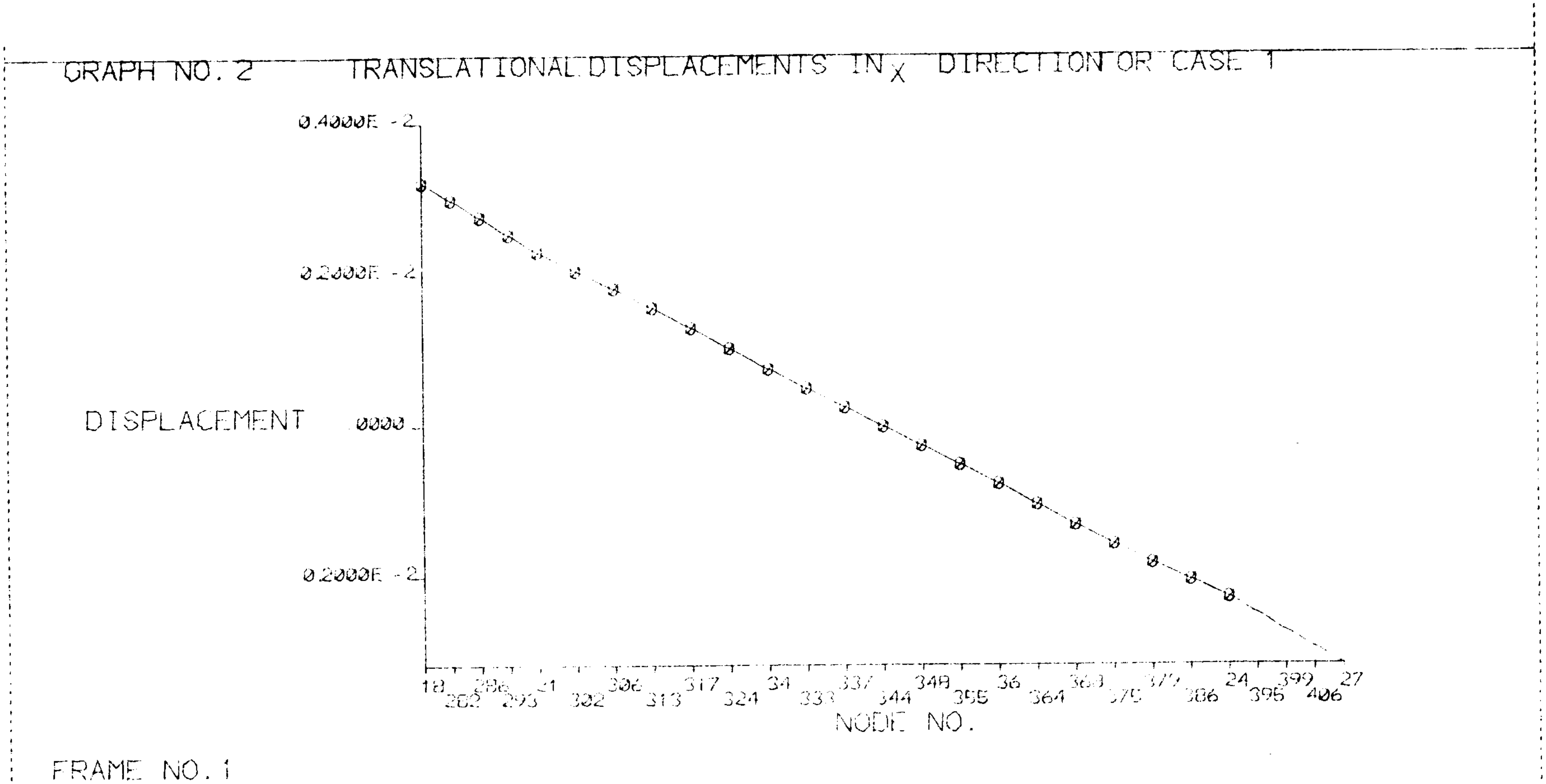

(b)

Figure 26 (continued)

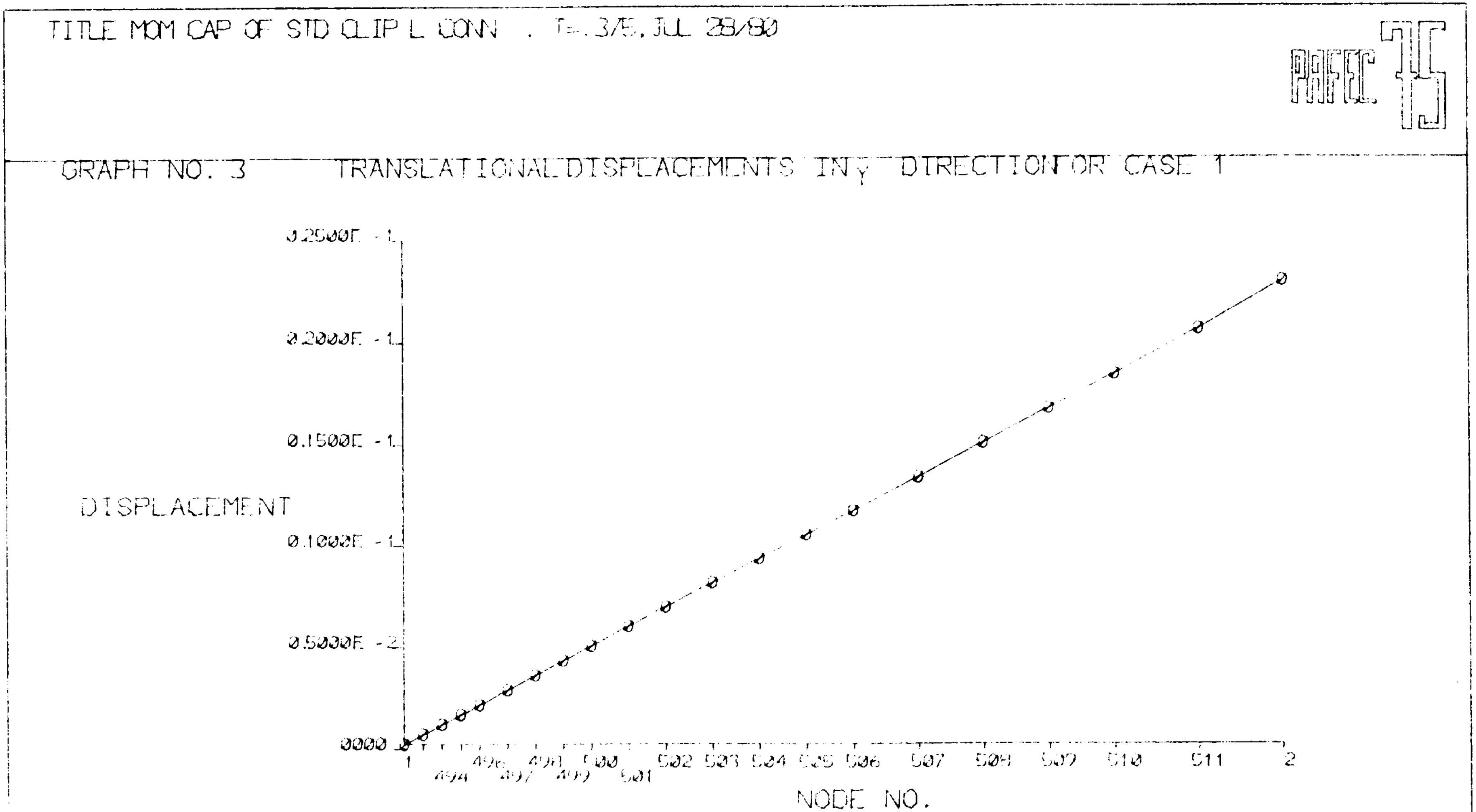

(a)

Figure 27. (a) Variation of U_y along Beam Bottom for t = 0.375"; (b) Variation of U_x along Beam End Just Beneath Angle for t = 0.375".

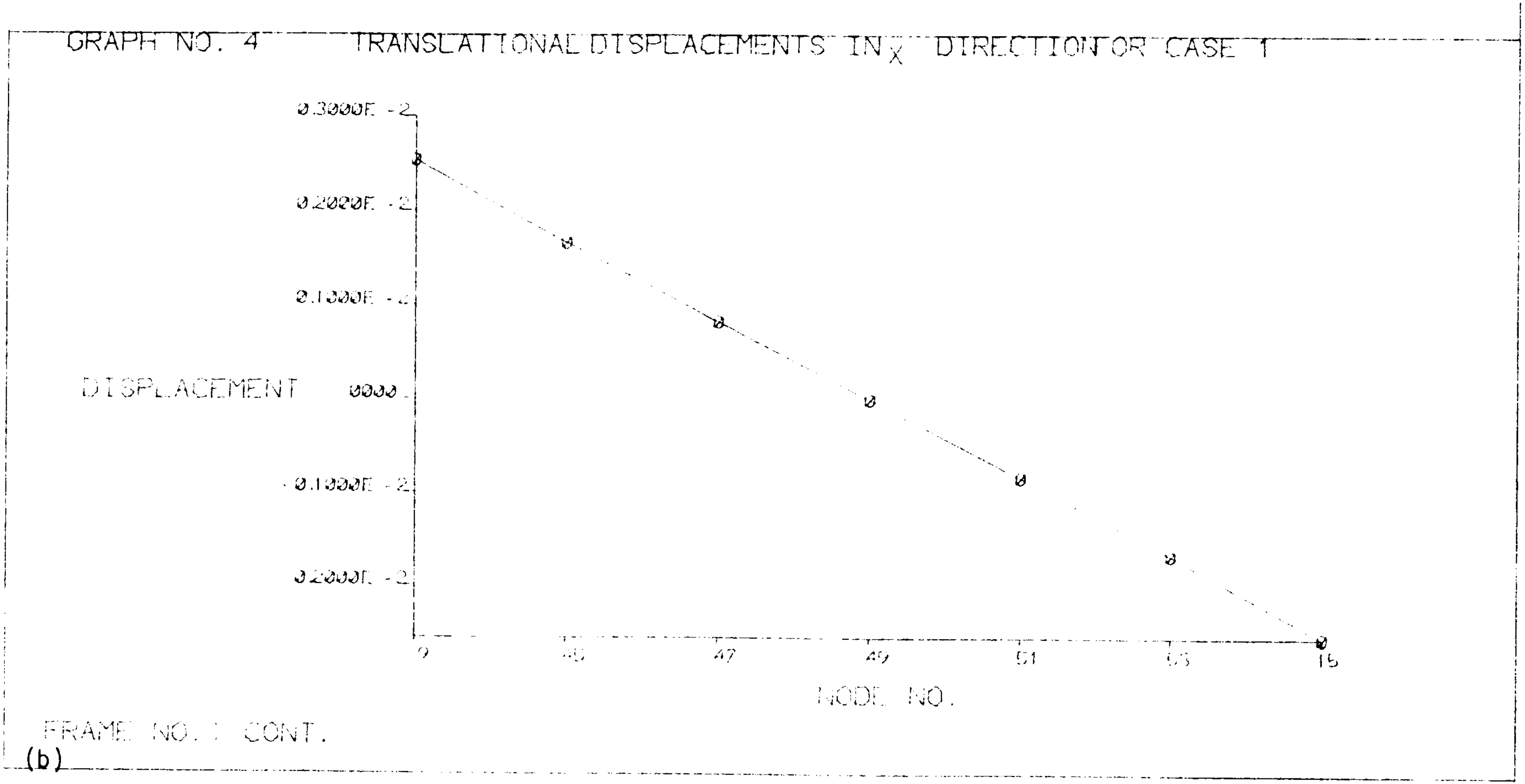

Figure 27 (continued)

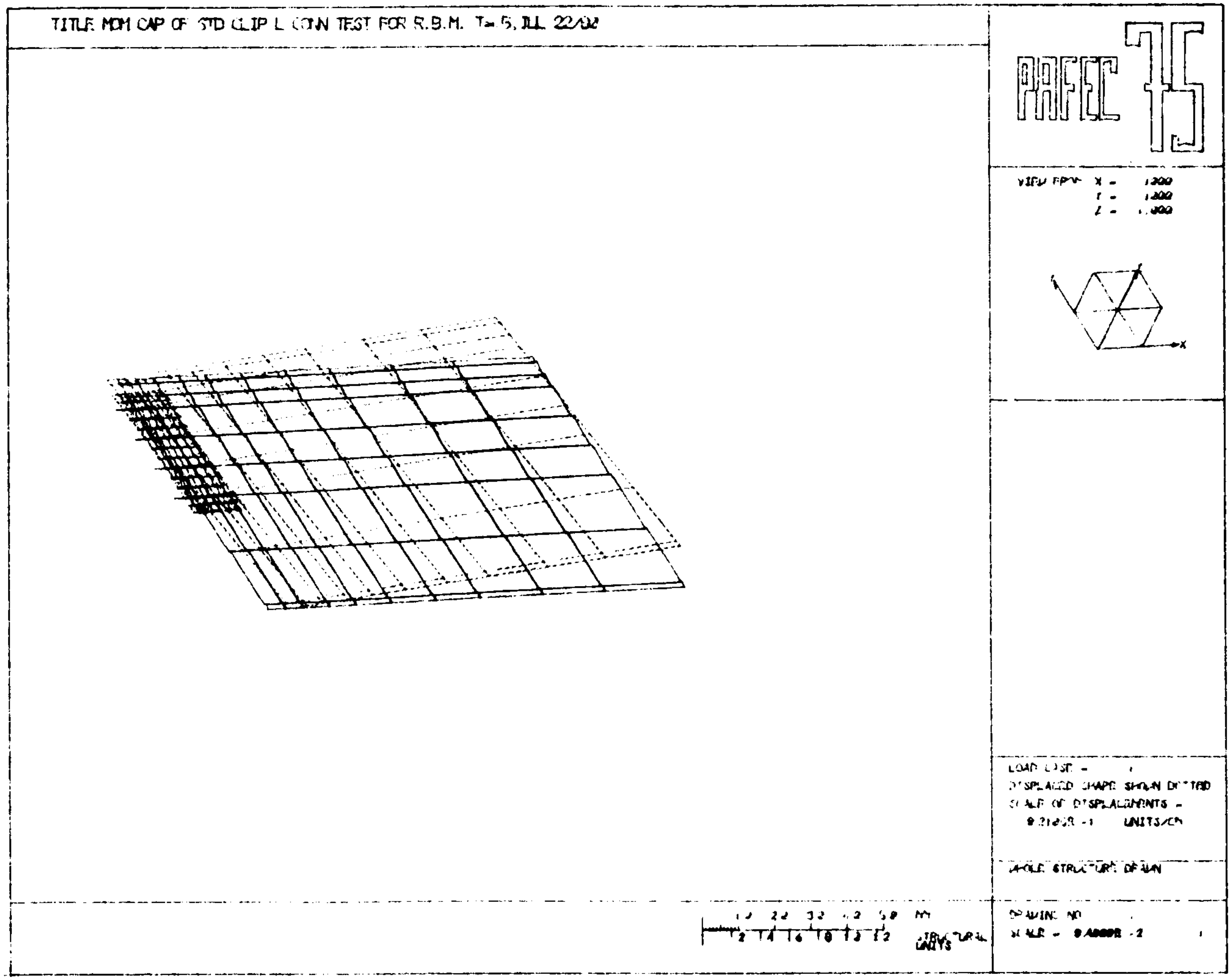

Figure 28. Isometric View of Displaced Shape for t = 0.500".

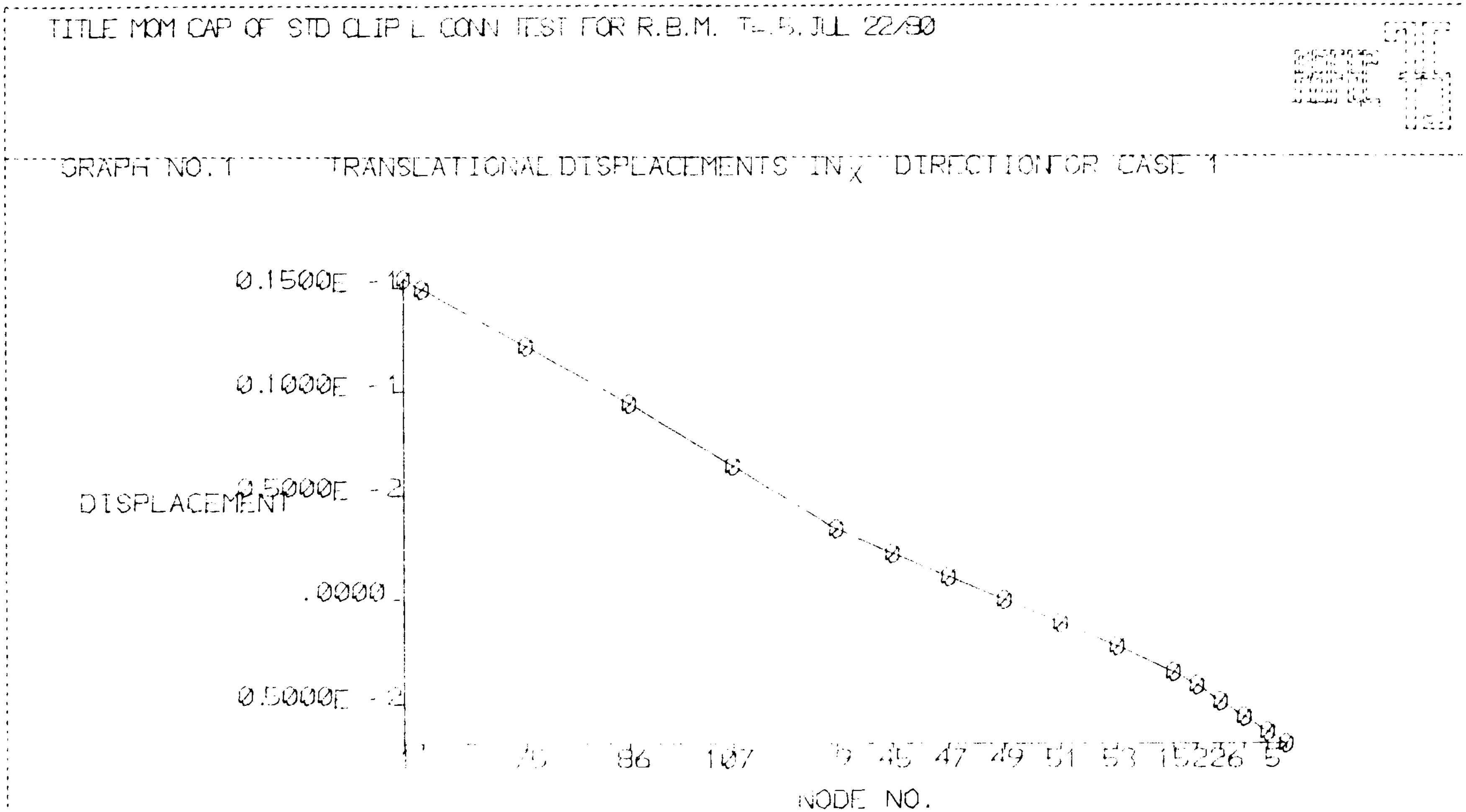

(a)

Figure 29. (a) Variation of U_x along Beam End for t = 0.5"; (b) Variation of U_x along Line Joining Web Bolts for t = 0.5".

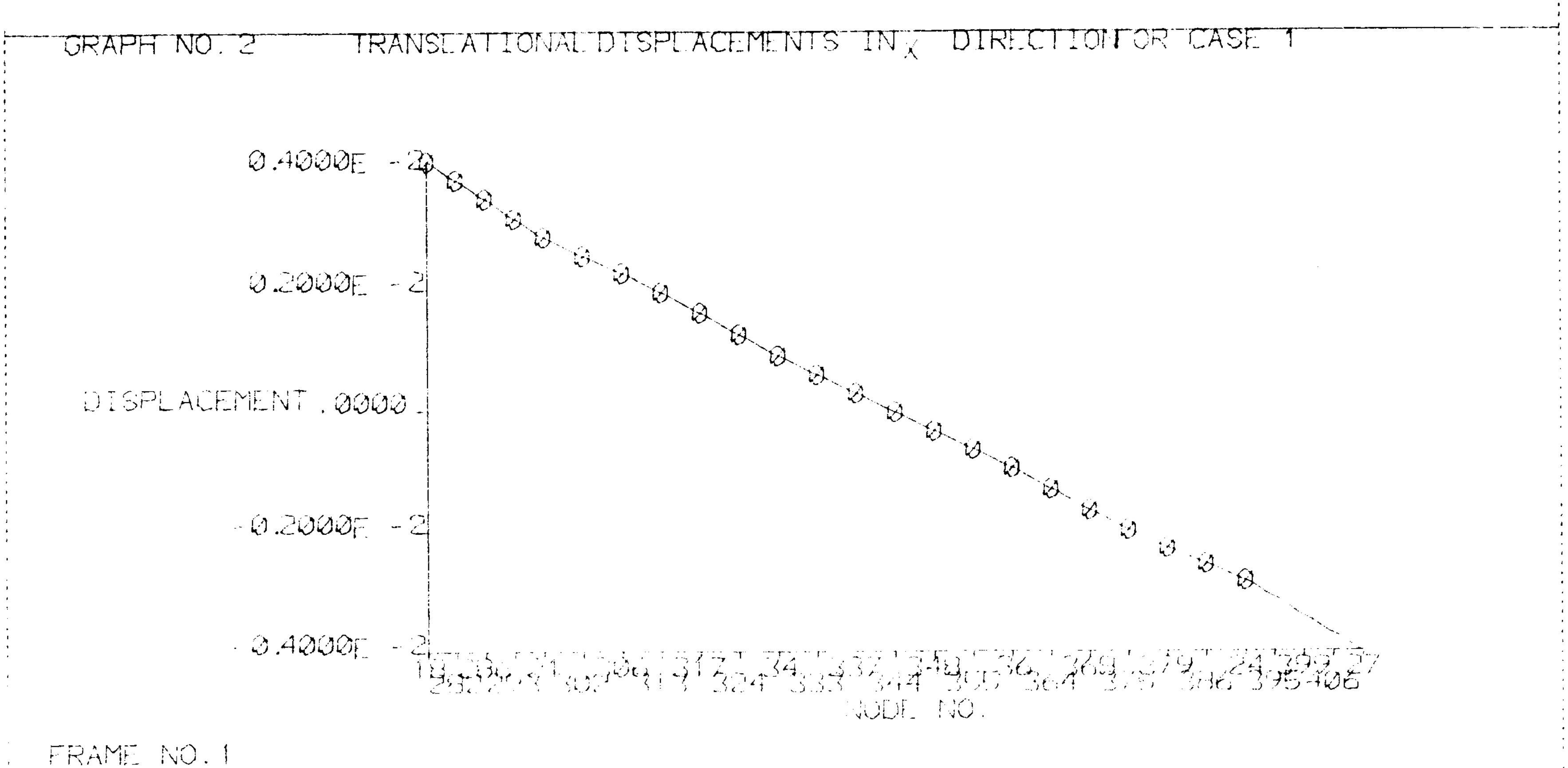

(b)

Figure 29 (continued)

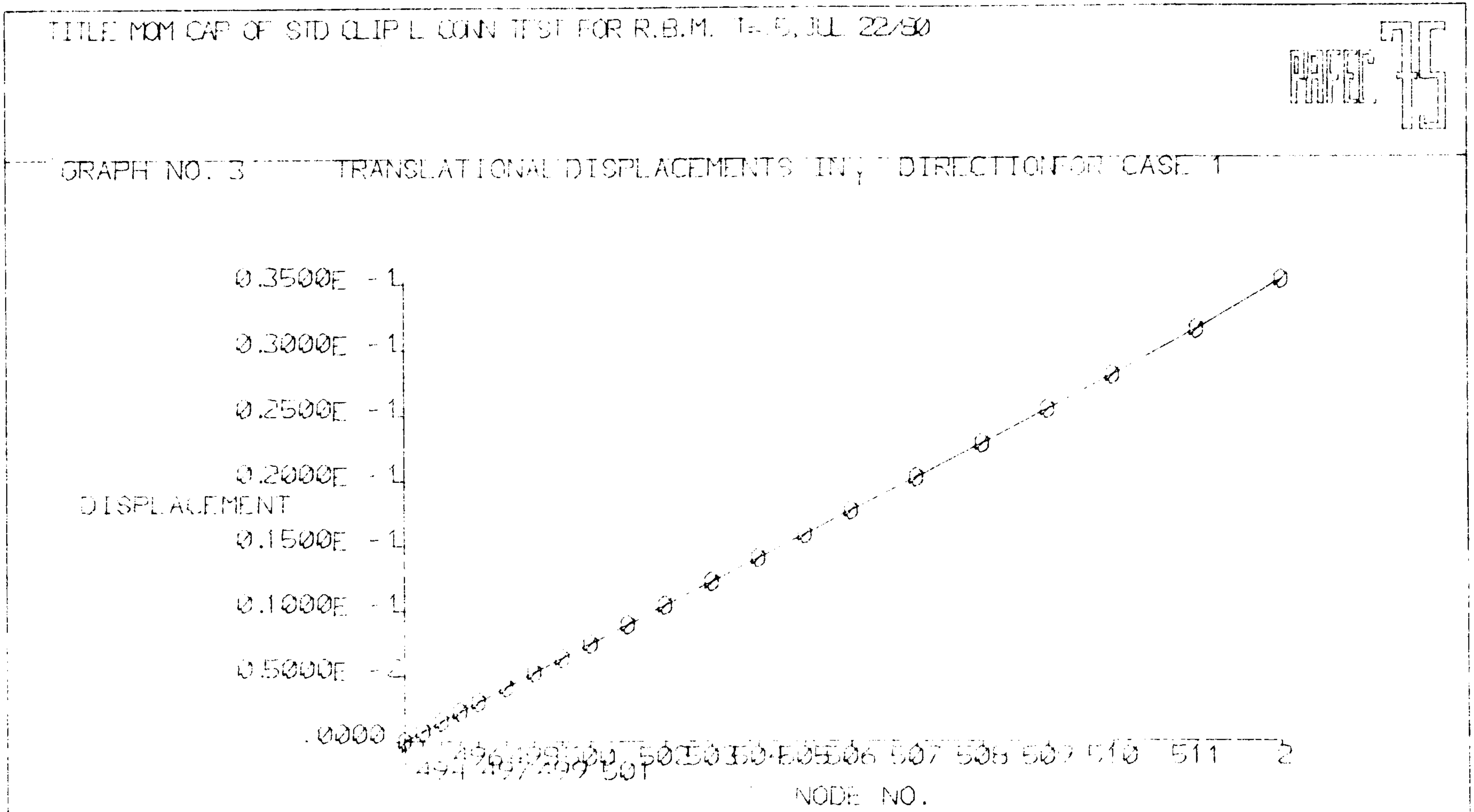

(a)

Figure 30. (a) Variation of U_y along Beam Bottom for t = 0.5"; (b) Variation of U_x along Beam End Just Beneath Angle for t = 0.5".

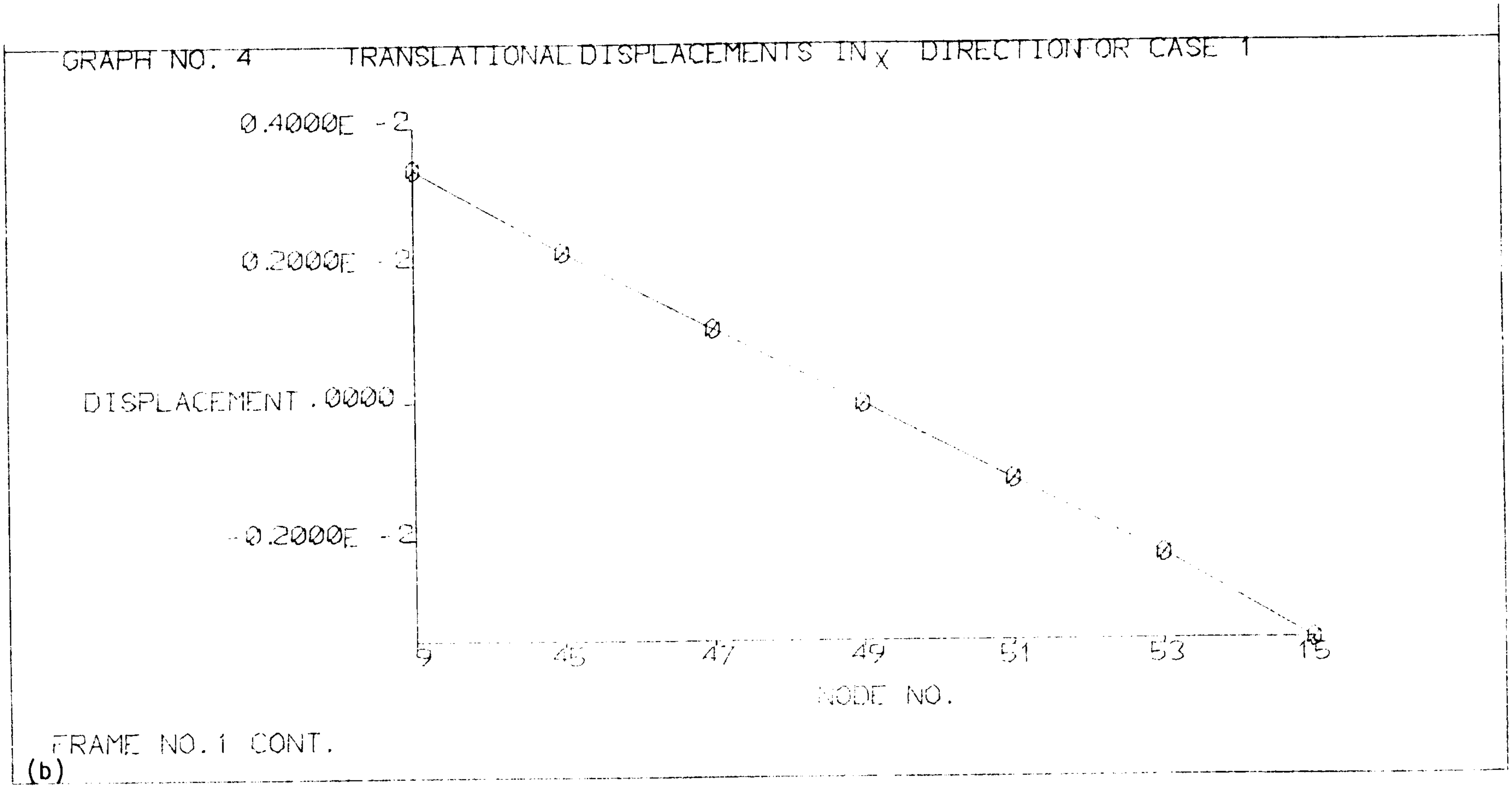

(b)

Figure 30 (continued)

TABLE 2

COMPARISON OF FINITE ELEMENT, EXPERIMENTAL AND THEORETICAL RESULTS

	Finite Element			Experimental			Theoretical		
	M_y kip-ft	$\phi_y \times 10^4$ rads	y in	M_y kip-ft	$\phi_y \times 10^4$ rads	y in	M_y kip-ft	$\phi_y \times 10^4$ rads	y in
t=0.250"	7.82	80.1	6.04	5.7	25.4	7.52	2.51	11.9	11.49
t=0.375"	11.24	37.0	6.12	9.6	23.91	7.84	5.73	7.1	11.24
t=0.500"	14.00	23.35	6.24	12.3	32.76	6.63	10.06	4.6	10.98

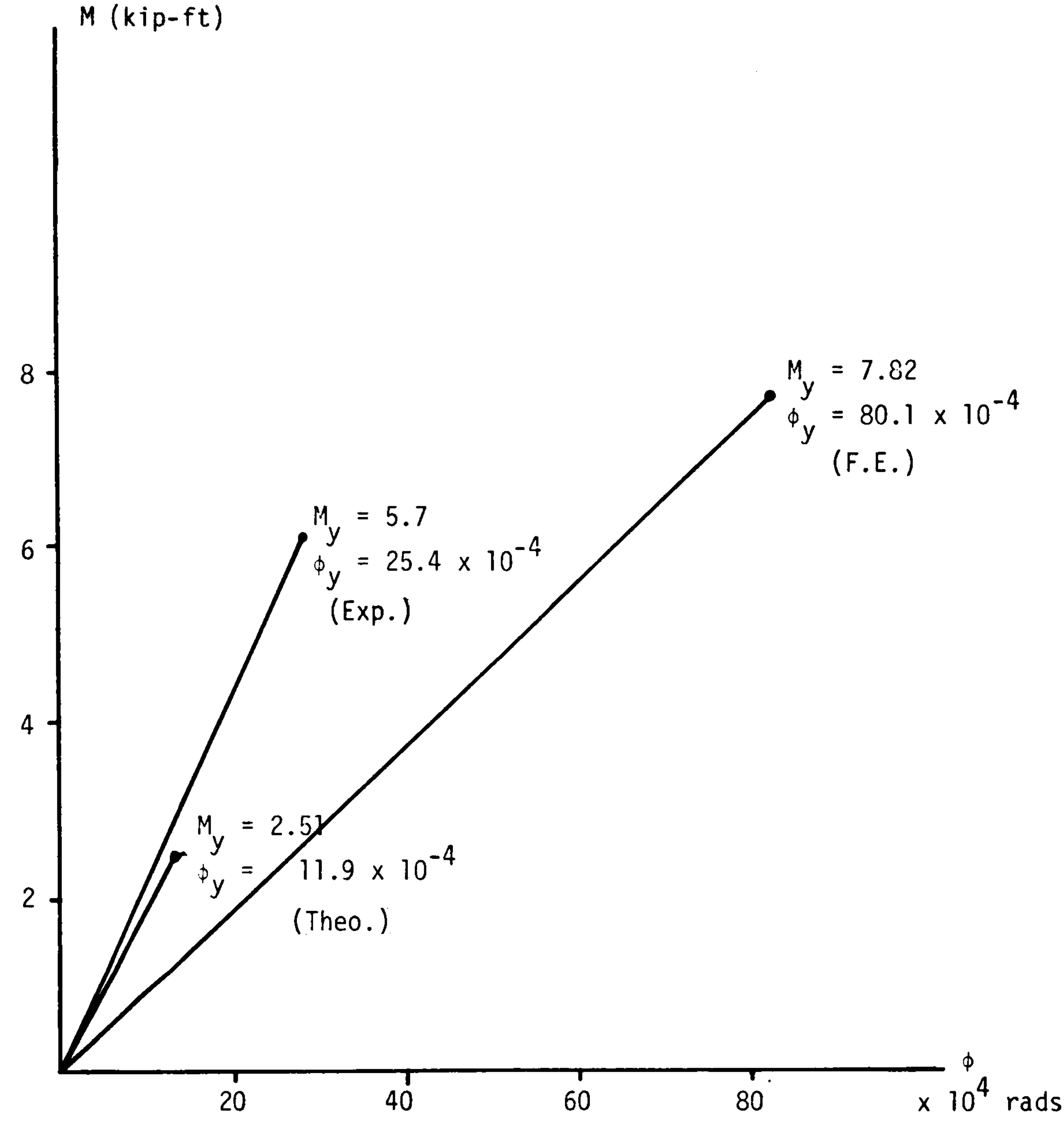

Figure 31. Moment-Rotation Curves for t = 0.25".

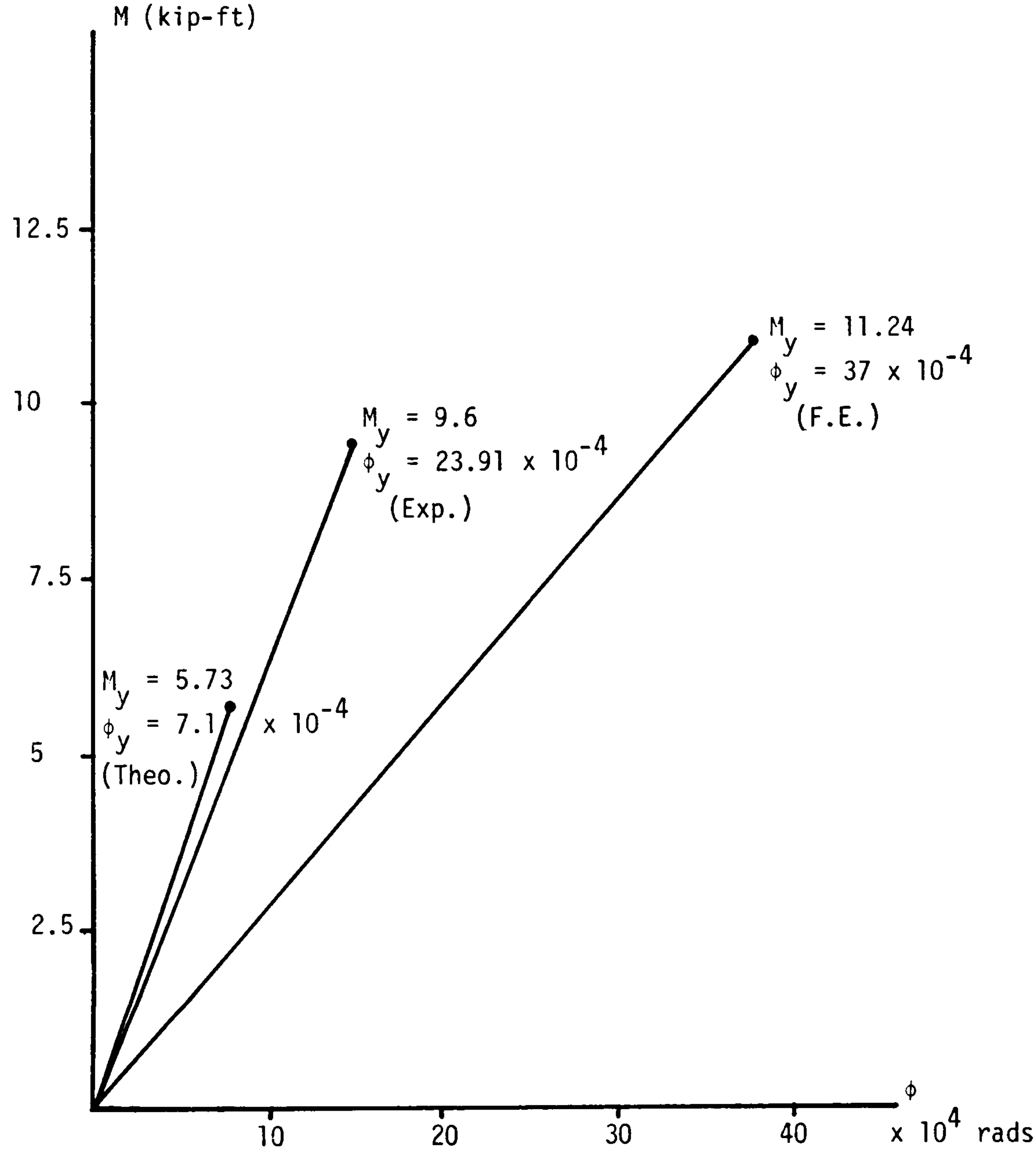

Figure 32. Moment-Rotation Curves for t = 0.375".

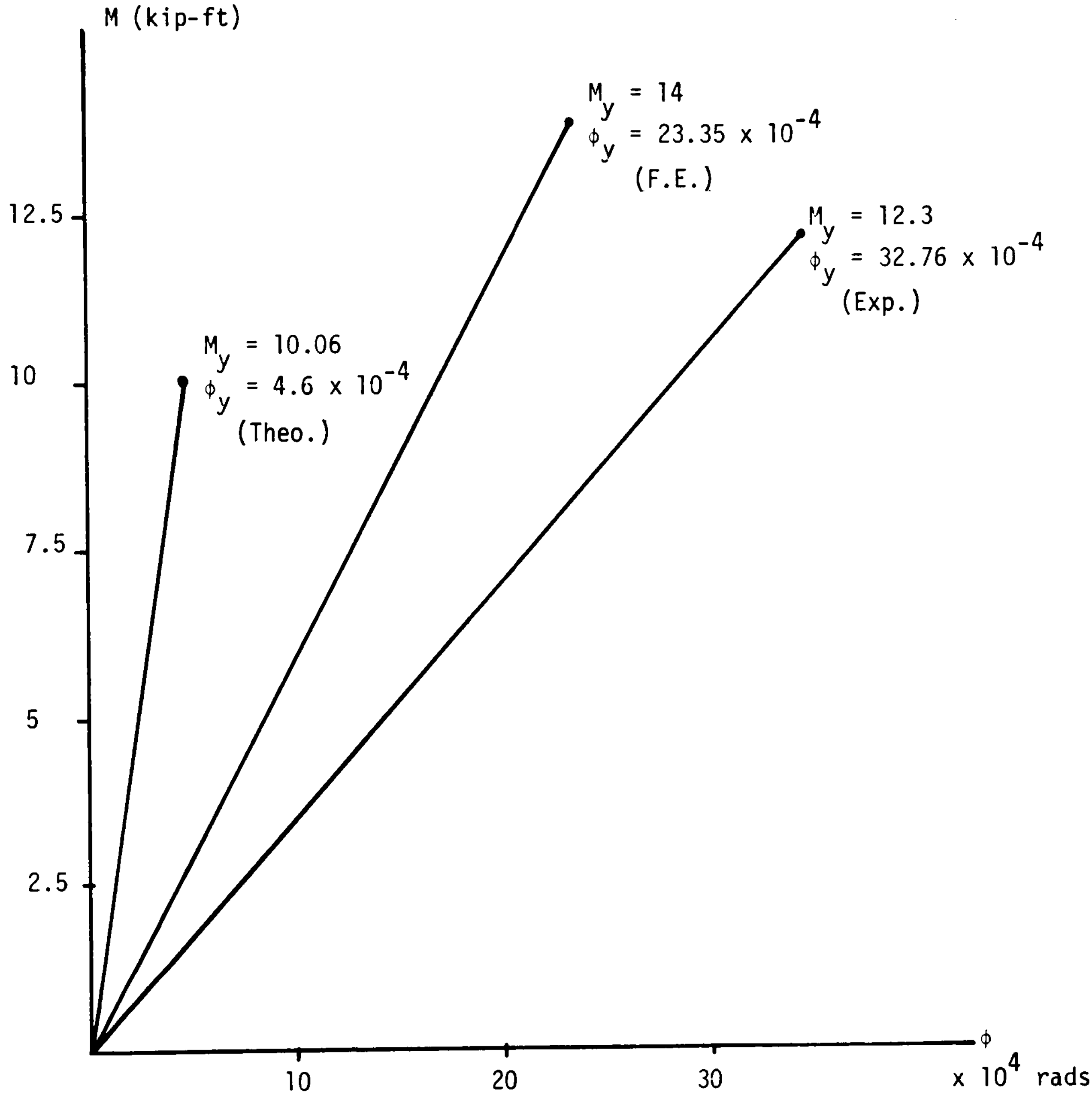

Figure 33. Moment-Rotation Curves for t = 0.500".

1. For all cases considered the yield moments, obtained by extrapolating finite element results, were higher than the theoretical yield moments predicted by Lothers' equations, as well as the observed experimental moments at yield. The extrapolated yield moments were higher than the observed ones by an average of 22.7 percent of those observed (37.2 percent higher for the 1/4" thickness and 13.8 percent higher for 1/2"). Since no information was available on the residual stress distribution in the tested specimens, steel was treated as an initially stress free material in the program. It was concluded that a residual stress distribution existed in the material tested. This distribution was different for the different thicknesses considered, being lowest for the 1/2" angle and highest for the 1/4" angle. The presence of such an initial stress distribution in the tested material lowered the value of the applied load that initiated yielding in the experiment.

2. For the lesser two thicknesses considered, yield rotations calculated from program output were found to be higher than their corresponding experimental results. For the 1/4" angle, the calculated ϕ_y was found higher than the experimental yield rotation by about 200 percent of the latter. The extrapolated yield rotation, for the 3/8" angle, was found to be higher than the experimental yield rotation by about 50 percent of the latter.

3. For the 1/2" thickness, the calculated ϕ_y was found less than the experimental yield rotation by approximately 30 percent of the experimental value. The experimental yield rotation for the 1/2" angle was higher than the experimental yield rotations of both the 1/4" and 3/8" angles (see Table 2, page 75).

Yield moments obtained from finite element output were expected to be higher than experimentally obtained values of the same quantity, due to residual stresses present, without further conclusions made on the overall connection behavior. However, the above cited differences between calculated and observed experimental yield rotations suggested inadequate modeling of the supports and therefore the resulting connection-support flexibility, as well as errors in the experimental investigation. While physical reasoning suggests that the thicker the angle the stiffer the connection, observed behavior indicated otherwise.

In the experimental investigation, the total flexibility of the connection was due to the lengthening of bolts, the distortion of the angle plate that framed into the column and the distortion of the column flange.

In the finite element model, the beam-column support was idealized by four springs, fixed at their column ends, each spring representing a bolt. The equivalent in-plane spring stiffness was determined as described in the preceding chapter. The method considered plate movement of the angle as well as bolt extension. The value so determined was dependent on angle thickness. As a result of this, the stiffness for the 1/2" angle was found to be an order of magnitude higher than that for the 1/4" angle and about twice that of the 3/8" angle. Bolt extensions were obtained by fixing the bolt end in the column flange. Since distortion of the column flange was not accounted for, the stiffness values used in the model were upper bound values for stiffnesses, within the limitations of the assumptions used in their derivation. This was verified by the results obtained from the finite element model for the 1/2" thickness.

The positions of the center of rotation, in the model, varied from 6.04" to 6.24" above the tension end of the angle. Those values indicated that the lower two bolts were in tension and the upper two bolts were in a compression contact zone for all three cases. Tensile and compressive forces in the bolts, due to the applied moment, balanced each other within 0.1 percent of the smallest spring reaction, thus ensuring horizontal equilibrium. The center of rotation at yield, in the experimental investigation, varied over a wider range of values. It was determined at 6.63" for the 1/2" angle indicating that the bolts in tension were equal to those in compression, at 8.52" for the 1/4" angle and at 7.84" for t = 3/8" (11). These values are summarized in Table 3 together with Lennon's determination of the position of the center of rotation from Lothers' equations.

TABLE 3

LOCATION OF CENTER OF ROTATION y FROM TENSION END OF ANGLE, NUMBER OF BOLTS IN TENSION (T) IN COMPRESSION (C)

Thickness (in)	Model			Experiment			Lothers		
	y	T	C	y	T	C	y	T	C
0.250	6.04	2	2	7.52	3	1	11.59	4	0
0.375	6.12	2	2	7.84	3	1	11.24	4	0
0.500	6.24	2	2	6.63	2	2	10.98	4	0

It was assumed that the closer the center of rotation was to the tension end of the angle, the larger the bearing area between the angle and the column. The compressive bearing stresses were assumed to vary from zero at the center of rotation to a maximum at the extreme compression fibers. This maximum extreme fiber stress was dependent on the number of bolts in tension. With a larger number of bolts in tension, the center of rotation was located higher. To ensure horizontal equilibrium, a higher stress gradient existed in a smaller bearing compression zone, where the plate of the angle reacted on the column flange. The smaller bearing area resulted in earlier yielding of the extreme angle fibers. This effect was reflected by the lower yield moments obtained by applying Lothers' theoretical equations and from Lennon's experimental results.

Comparison of yield rotations indicated that the spring stiffnesses used in the model resulted in a more flexible connection when the angle thicknesses of 1/4" and 3/8" were considered. The finite element model resulted in a stiffer connection when the angle thickness was 1/2". This was reflected by a rotation at yield smaller than the corresponding experimental rotation. Figure 34 shows finite element and experimental M-ϕ curves plotted to the same scale. From this figure it was observed that the experimental stiffness for the 1/2" angle was less than the experimental stiffness of the 3/8" as well as the 1/4" angle, although the larger the angle stiffness the stiffer the connection should have been. This variation of yield rotation with stiffness was observed in the finite element results. Figure 35 shows the finite element and theoretical M-ϕ curves plotted to the same scale. In this figure increase in stiffness with increase in angle thickness was observed by both finite element and theoretical calculations.

The bolt ends in the column flange were considered fixed when flexibility due to bolt elongation was calculated. As a result, distortion of the column flange was zero, resulting in a connection

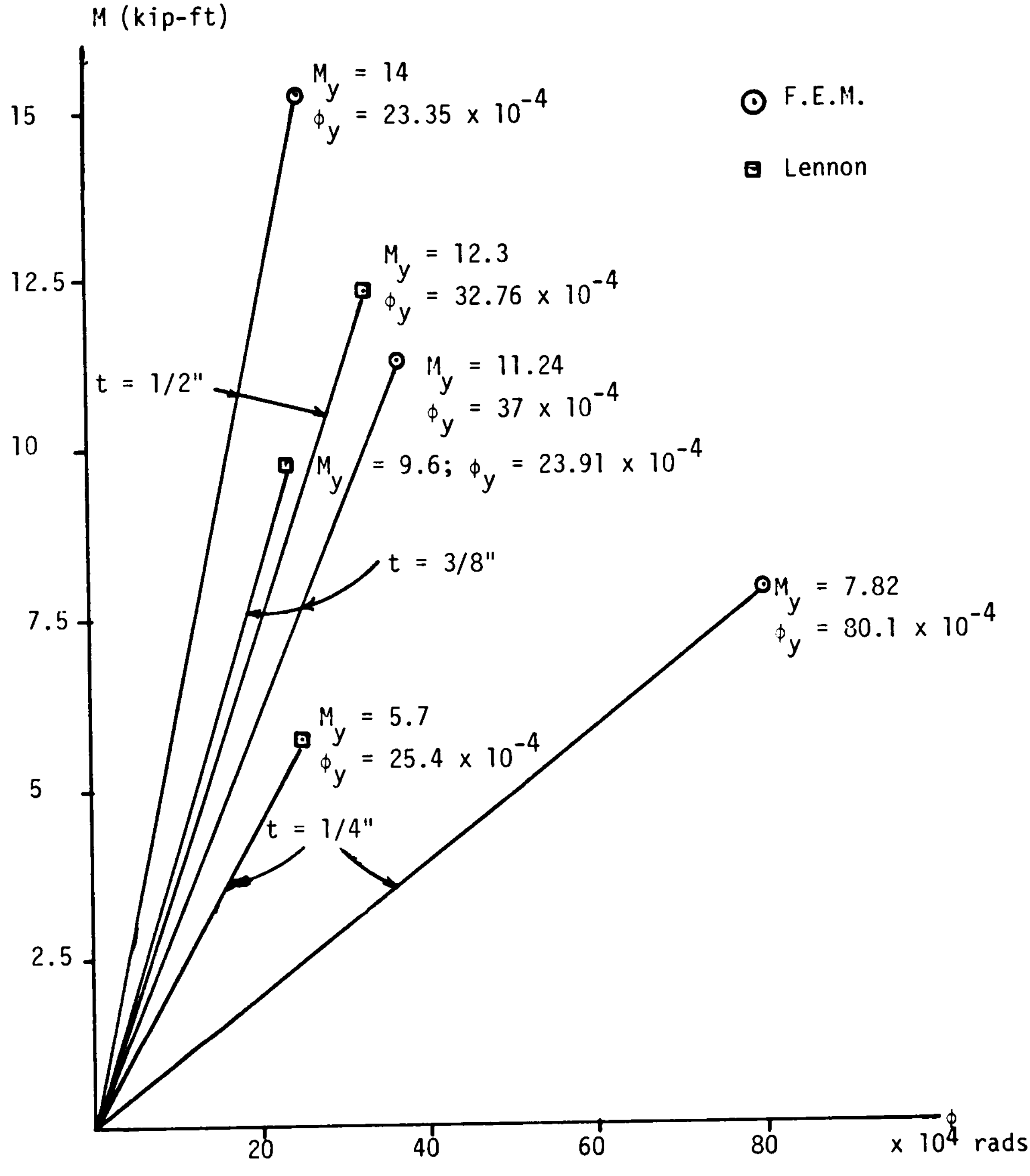

Figure 34. Comparison of Finite Element and Experimental M-ϕ Curves.

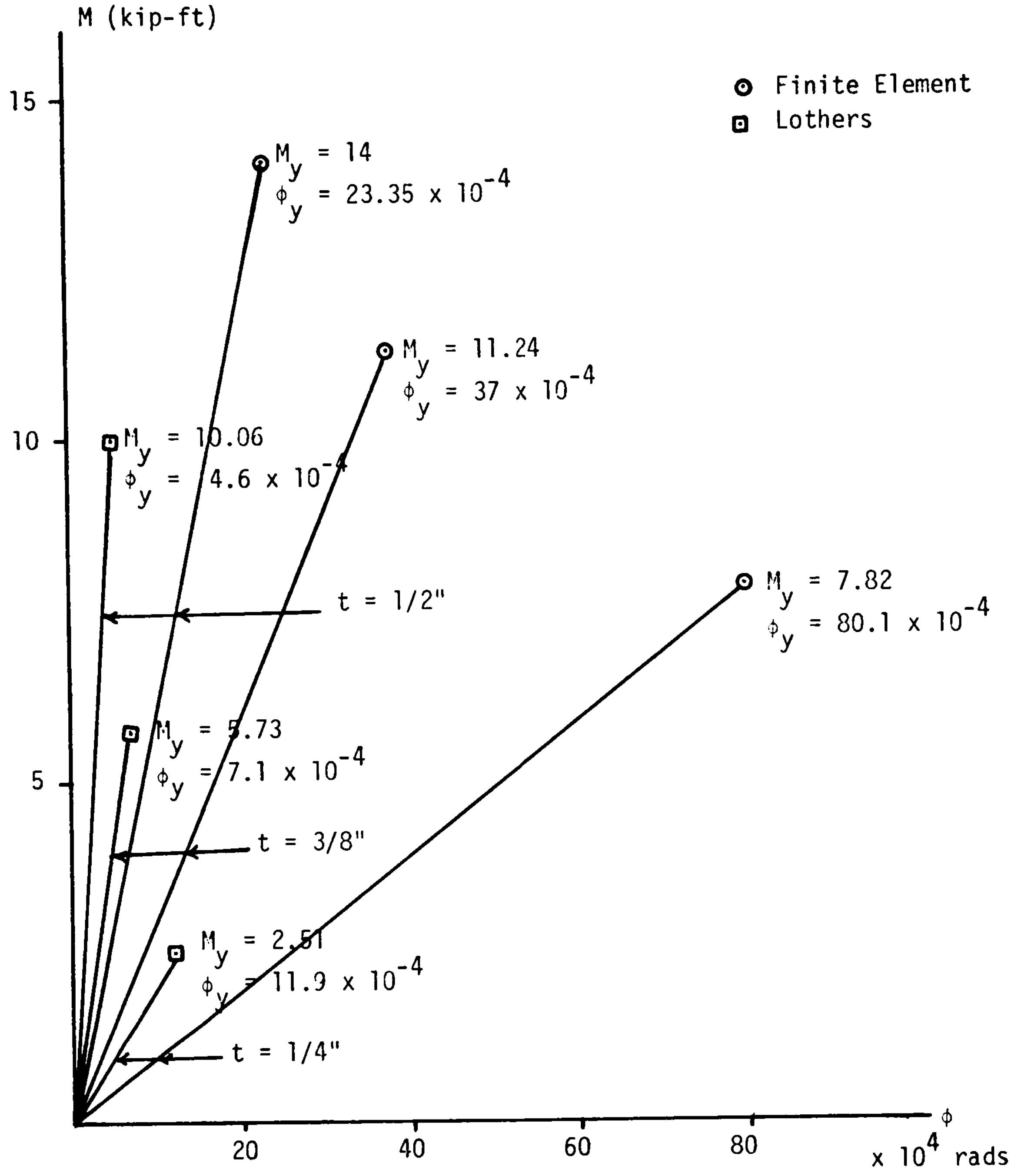

Figure 35. Comparison of Finite Element M-ϕ Curves and M-ϕ Curves from Lothers' Theoretical Equations.

stiffer than the experimental connection where plate distortion occurred. This was observed for the 1/2" angle only, where the calculated stiffness provided an upper bound value for the stiffness of the connection. Experimental values obtained for ϕ_y for the smaller two thicknesses suggested equipment error dominating the difference in results when compared with computer round-off error.

In deriving the equivalent bolt stiffness as shown in Figure 16 (page 45), joint B was not allowed to rotate. If this joint is allowed to do so the equivalent spring stiffnesses would be lower. A derivation is made below (Figure 36) for the case considering plate movement only. This result can be extended to the case where both plate movement and bolt elongation are considered. Figure 36(a) shows the angle portion between the two bolt lines and fixed at those bolt lines, and acted upon by a load P, whose line of action is along BC. P is the total shear taken by the four bolts connecting the angle to the column. Those bolts are assumed to take equal shears. The load P causes a displacement Δ as shown in Figure 36(b), which also shows the final displaced shape of the angle taking into account the rotation of joint B. The displacement Δ induces equal fixed end moments M, of $\frac{6EI\Delta}{L^2}$ at A and B, as seen in Figure 36(c). Figure 36(d) shows final distributed moments in the structure. To obtain equivalent bolt stiffnesses, K_{eg}, a free body diagram of segment AB is shown in Figure 36(e) with the final moments and shears acting. From Figure 36(e), we have

$$P = \frac{7.5\ EI\Delta}{L^3} \qquad \text{(i)}$$

$$F_{bolt} = K_{bolt} \cdot \Delta \ . \qquad \text{(ii)}$$

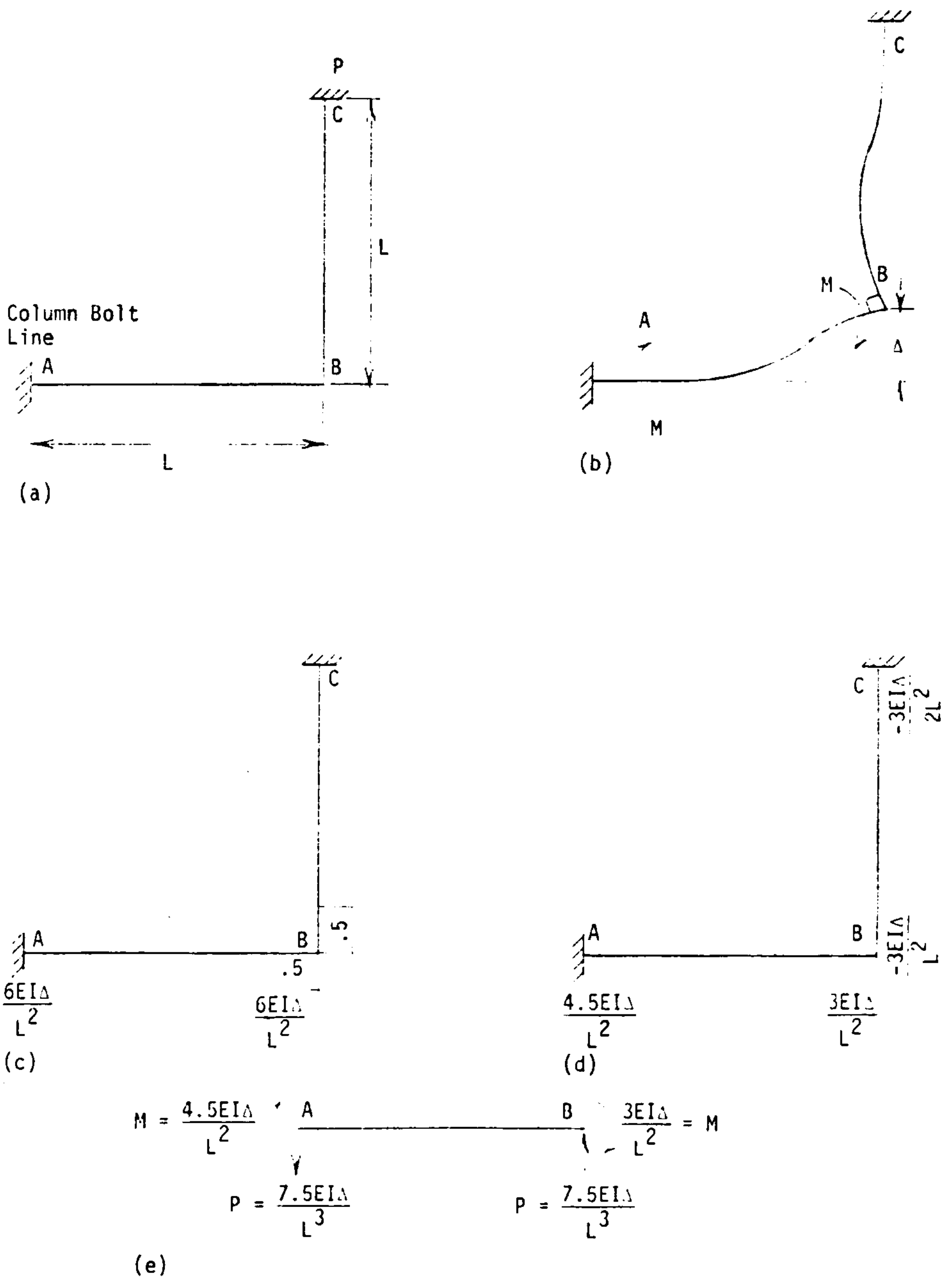

Figure 36. Alternative Derivation of Equivalent Bolt and Angle Stiffness Showing (a) Undisplaced Shape; (b) Displaced Shape; (c) Fixed-End Moments Due to Displacement Δ; (d) Final Distributed Moments; (e) Final Moments and Shears on AB.

Since it was assumed that the four bolts resist the shear equally, then

$$P = 4 \times F_{bolt} . \qquad \text{(iii)}$$

Substituting for P (Eq. iii) and F_{bolt} (Eq. ii) into Eq. (i)

$$\frac{7.5\ EI\Delta}{L^3} = 4 \times K_{bolt} \times \Delta.$$

Solving for K_{bolt} yields

$$K_{bolt} = \frac{15}{8} \frac{EI}{L^3} . \qquad (30)$$

Extending the result to the case where bolt elongation is considered

$$\frac{1}{K_{eq}} = \frac{L}{AE} + \frac{8}{15} \frac{L^3}{EI} . \qquad (31)$$

CHAPTER VI

CONCLUSIONS AND RECOMMENDATIONS

I. CONCLUSIONS

A major objective of this study was to obtain Moment-rotation characteristics of simple beam connections by the finite element method. Another objective of this investigation was to compare the characteristics so obtained with the experimentally observed elastic behavior as well as the predicted theoretical behavior of the same connections. The behavior of the latter two were obtained and compared by Lennon (11).

Yield moment and yield rotation were used as a basis for the comparison. The following differences between finite element, experimental and theoretical values for the yield rotation ϕ_y, and yield moment, M_y, were observed:

1. For all thicknesses considered M_y, as calculated from finite element output, was higher than both experimental and theoretical values obtained.

2. The calculated rotations, ϕ_y, were larger than the values obtained by Lennon in both his experiments and his calculations of ϕ_y from Lothers' theoretical equations when the angle thicknesses were 1/4" and 3/8".

3. For the 1/2" angle, yield rotation was calculated from the finite element program output and was found to be larger than the predicted theoretical ϕ_y and less than that observed by Lennon.

Those differences were believed to have been influenced by

a. Not accounting for residual stresses in the finite element model due to lack of information on the distribution of such stresses. Thus an initial stress free state was assumed.

b. Modeling the flexibility of the connection. The total connection flexibility was due to the following:

(i) Bolt extension.

(ii) Distortion of the angle leg that framed into the column.

(iii) Plate distortion of the column flange.

While plate distortion of the column flange was not accounted for, the stiffness values so determined were upper bound values, within the limitations of the derivation. This is true since the addition of column flange distortion adds to the flexibility and thereby reduces the stiffness of the connection. Thus the existence of a compression contact zone between the angle and column reduced stiffness since this decreased the number of bolts in tension. This was observed in all results.

The values obtained for M_y were consistently higher than experimental and theoretical values for all cases considered. This increase in the value of M_y was due to the assumption that no residual stresses existed in the material, as well as the higher stress gradient that existed in the compression contact zone between angle and column due to a smaller compression area as determined from the position of the center of rotation.

Values obtained for ϕ_y from computer output showed an increase in connection stiffness with increase in angle thickness. The same variation was obtained by Lennon from Lothers' equations. Experimentally observed behavior showed that the 1/2" angle was more flexible than the

1/4" or the 3/8" angle. Since a thicker angle results in a stiffer connection it was concluded that the values obtained for the latter two thicknesses were the result of equipment error. The connection stiffness used in the model was an upper bound value for stiffness. This was verified by comparing the values of yield rotations from both finite element and experimental methods.

II. RECOMMENDATIONS

It is suggested that the following be made in future investigations of simple connections by the finite element method.

1. Have a plate bending model of the part of the column flange underneath this angle leg and between stiffeners used, with the bolts as points of load application. From this model, contribution to flexibility of column flange distortion can be estimated thus giving a better estimate of the total overall connection flexibility.

2. Obtain load-extension curves for the bolts from bolt calibration tests as was done by Nair, Birkemoe and Munse (17). Such curves give an estimate of the change of elastic properties in the inelastic zone.

3. Include in the estimate of bolt stiffness the rotation of point B, i.e., use Eqs. 30 and 31.

4. Fix top mode(s) on the angle leg framing into the column to stimulate the effect of a compression contact zone.

5. Include the inelastic behavior to compare values above the yield stress level.

LIST OF REFERENCES

LIST OF REFERENCES

1. Akin, J. E., Application and Implementation of the Finite Element Method, Academic Press, London, 1980.

2. American Institute of Steel Construction, Manual of Steel Construction, Seventh Edition, AISC, New York, 1970.

3. Bathe, K. J., and Wilson, E. L., Numerical Methods in Finite Element Analysis, Prentice-Hall, Englewood Cliffs, New Jersey, 1976.

4. Driscoll, G. C., "Effective Length of Columns with Semi-Rigid Connections," AISC Engineering Journal, Vol. 13, No. 4, Fourth Quarter, 1976.

5. Ergatoudis, I., Irons, B. M., and Zienkiewicz, O. C., "Curved, Isoparametric, 'Quadrilateral' Elements for Finite Element Analysis," International Journal of Solids and Structures, Vol. 4, 1968.

6. Fisher, J. H., and Struik, J. H. A., Guide to Design Criteria for Bolted and Riveted Joints, Wiley-Interscience, New York, 1974.

7. Hinton, E., and Owen, D. R. J., Finite Element Programming, Academic Press, London, 1977.

8. Huebner, K. H., The Finite Element Method for Engineers, Wiley-Interscience, New York, 1975.

9. Krishnamurthy, N., and Graddy, D. E., "Correlation between 2- and 3-Dimensional Finite Element Analysis of Steel Bolted End-Plate Connections," Computers and Structures, Vol. 6, Pergamon Press, London, 1976.

10. Krishnamurthy, N., "A Fresh Look at Bolted End-Plate Behavior and Design," AISC Engineering Journal, Vol. 17, No. 2, Second Quarter, 1978.

11. Krishnamurthy, N., Huang, H. T., Jeffrey, P. K., and Avery, L. K., "Analytical M-θ Curves for End-Plate Connections," Proceedings, ASCE, Vol. 105, ST1, January 1979.

12. Lennon, K., "Comparison of Observed and Predicted Elastic Behavior of AISC Standard Framed Beam Connections," Master's Thesis, The University of Tennessee, Knoxville, 1980.

13. Livesley, R. K., Matrix Methods of Structural Analysis, Second Edition, Pergamon Press, Oxford, 1975.

14. Lothers, J. E., Advanced Design in Structural Steel, Prentice-Hall Englewood Cliffs, New Jersey, 1960.

15. Munse, W. H., "Research on Bolted Connections," Transactions of the American Society of Civil Engineers, Vol. 121, ASCE, New York, 1956.

16. Munse, W. H., Bell, W. G., and Chesson, E., "Behavior of Riveted and Bolted Beam-to-Column Connections, Proceedings, ASCE, ST3, New York, March 1959.

17. Nair, R. S., Birkemoe, P. C., and Munse, W. H., "High Strength Bolts Subject to Tension and Prying," Proceedings, ASCE, Vol. 100, ST2, New York, February 1974.

18. PAFEC, PAFEC 75 Data Preparation, PAFEC Ltd., Nottingham, 1978.

19. Rathbun, J. C., "Elastic Properties of Riveted Connections," Transactions, ASCE, Vol. 101, 1936.

20. Salmon, C. G., and Johnson, J. E., Steel Structures: Design and Behavior, Intext Educational Publishers, New York, 1971.

21. Tong, P., and Rossettos, J. N., Finite-Element Method, M.I.T. Press, Cambridge, Mass., 1977.

22. Zienkiewicz, O. C., The Finite Element Method, Third Edition, McGraw-Hill Book Co. (UK) Limited, England, 1977.

APPENDIX

APPENDIX

DATA FILES USED FOR RUNNING PAFEC

For Half-Inch Angle Thickness

```
CONTROL
NAME.T500
FAST.READ
FULL.CONTROL
PHASE=1
PHASE=2
PHASE=4
SAVE
SAVE.FILES
PHASE=6
BASE=27500
SAVE
SAVE.FILES
PHASE=7
BASE=38000
SAVE.FILES
SAVE.DISPS
STOP
PHASE=8
BASE=35000
PHASE=9
BASE=35000
CONTROL.END
TITLE MOM CAP OF STD CLIP L CONN,T=0.5,JUL 22/80
NODES
NODE      X      Y      Z
C W-SECTION
C LOWER FLANGE
1         0.0    0.0
C NODE FOR LOAD APPLICATION,CUTTING LAST SEGMENT OF BEAM
2         35.25   0.0
3          0.0    0.5
4         35.25   0.5
C UPPER FLANGE
5          0.0   23.0
6         35.25  23.0
7          0.0   23.5
8         35.25  23.5
```

```
C ROW OF FASTENER BOLTS
10        1.50  11.5
12        1.50  14.5
13        1.50  17.5
14        1.5   20.5
C OTHER NODES IN WEB FOR TOPOLOGICAL DESCRIPTION
9         0.0   11.5
11       35.25  11.5
15        0.0   20.5
16       35.25  20.5
C ANGLE
C FASTENER BOLTS
29        1.51  11.5
30        1.51  14.5
31        1.51  17.5
32        1.51  20.5
C OUTSTANDING LEG
17       -0.75  10.0
20       -0.75  11.5
23       -0.75  20.5
26       -0.75  22.0
C OTHER NODES IN ANGLE FOR TOPOLOGICAL DESCRIPTION
19        3.25  10.0
22        3.25  11.5
25        3.25  20.5
28        3.25  22.0
33       -0.75  14.5
35       -0.75  17.5
38          1.51  10
39        1.51   22
C X- COORDINATE HAS TO BE CHANGED WITH EACH NEW THICKNESS
C X-COORD=-.75+THICK
36       -0.250 17.5
34       -0.250 14.5
27       -0.250 22.0
24       -0.250 20.5
21       -0.250 11.5
18       -0.250 10.0
C ADDITIONAL NODES FOR SPRINGS
C ATTACH TO SPRING AND GROUND WHEN SPRING HAS FINITE LENGTH
37      -1.75  11.5
40      -1.75  14.5
41      -1.75  17.5
42      -1.75  20.5
C ADD NODE ALONG Z-AXIS FOR VIEW OF DISPLACED SHAPE
43          0       0       100000
ELEMENTS
ELEMENT.TYPE=30100
GROUP=1
PROP=4
NUMBER    TOPO
1       20  37
2       33  40
```

```
3         35   41
4         23   42
PAFBLOCKS
TYPE=1
ELEMS.ARE.8.NODE.QUADS=36210
GROUP       PROP       N1       N2       TOPOLOGY
C WEB
11          2          4        5        9  10 15 14
13          2          1        3        3  4  9  11
14          2          6        5        10 11 14 16
15          2          1        7        15 16 5  6
C ANGLE WEB ELEMENTS
5           4          13       10       18 38 21 29
6           4          13       12       21 29 24 32
7           4          13       15       24 32 27 39
8           4          14       10       38 19 29 22
9           4          14       12       29 22 32 25
10          4          14       15       32 25 39 28
PAFBLOCKS
TYPE=10
ELEMS.ARE.6.NODE.QUADS=36240
GROUP       PROP       N1       TOPOLOGY
C FLANGES
12          1          1        1  2  3  4
16          1          1        5  6  7  8
PAFBLOCKS
TYPE=1
ELEMS.ARE.8.NODE.QUADS=36210
GROUP       PROP       N1       N2       TOPOLOGY
C ANGLE COLUMN ELEMENTS
2           3          9        12       20 21 23 24
3           3          9        10       17 18 20 21
4           3          9        15       23 24 26 27
MESH.SPACING
REFER.TO.N1.OR.N2      SPACING.RATIO.OR.NO.OF.ELEM
1                      2  2  3  3  4  5  5  7  7  9
2                      1
3                      2
4                      1
5                      3
6                      2  3  3  4  5  5  7  7  9
7                      2
8                      1
9                      1
10                     2
12                     9
13                     3
14                     2
15                     2
```

```
MATERIALS
MATERIAL.NO       E          NU
1                 29E6       0.3
PLATES.AND.SHELLS
MATERIAL.NUMBER=1
PLATE.NUMBER      THICKNESS
1                 3.5
2                 0.1875
3                 2.0
C THICKNESS TO BE CHANGED
4                 0.500
SPRINGS
NUMBER.OF.SPRINGS      KX
4                       1.229E6
STRESS.ELEMENTS
GROUP
2
3
4
5
6
7
8
9
10
DISPLACEMENTS.PRESCRIBED
NODE    DIRE    DISP.VALU    LOAD.CASE
2       2        0.03525      1
REPEATED.FREEDOMS
DIRE=12
N1    N2
10    29
12    30
13    31
14    32
GRAPH.OF.DISPLACEMENTS
TYPE    LIST.OF.NODES
C  X-DISP ALONG X=0
1       1    7
C  X DISP ALONG X=-0.25
1       18   27
C  Y DISP OF LOWER FLANGE
2       1    2
C  X DISP ALONG X=0 JUST BENEATH ANGLE
1       9    15
RESTRAINTS
NODE    PLANE    DIRE
C  RESTRAIN TO PLANE PROBLEM
1       3        3456
```

```
C  RESTRAIN BOTTOM BOLT FROM VERTICAL DISPLACEMENT
C OTHERWISE A MECHANISM MAY FORM IE RIGID BODY MOTION
20      0       2
C  ADD NODES TIED TO SPRINGS
37      0       0
40      0       0
41      0       0
42      0      0
OUT.DRAW
PLOT    GROUPS
1       0
REACTIONS
C  REPLACE REACTIONS IN C M TO ONLY ACTIVE NODES
C  IE AT CONSTRAINTS AND AT PRES DISPS
NODES
2
20
23
37
40
41
42
END.OF.DATA
```

For Three-Eighths Inch Angle Thickness

```
CONTROL
NAME.T375
FAST.READ
FULL.CONTROL
PHASE=1
PHASE=2
PHASE=4
PHASE=6
BASE=27500
SAVE
SAVE.FILES
PHASE=7
BASE=38000
SAVE.FILES
SAVE.DISPS
PHASE=8
BASE=38000
PHASE=9
BASE=38000
PHASE=10
BASE=38000
CONTROL.END
TITLE MOM CAP OF STD CLIP L CONN  , T=.375,JUL 28/80
NODES
NODE      X      Y      Z
C W-SECTION
C LOWER FLANGE
1          0.0    0.0
C NODE FOR LOAD APPLICATION,CUTTING LAST SEGMENT OF BEAM
2         35.25    0.0
3          0.0    0.5
4         35.25    0.5
C UPPER FLANGE
5          0.0   23.0
6         35.25   23.0
7          0.0   23.5
8         35.25   23.5
C ROW OF FASTENER BOLTS
10         1.50   11.5
12         1.50   14.5
13         1.50   17.5
14         1.5    20.5
C OTHER NODES IN WEB FOR TOPOLOGICAL DESCRIPTION
9          0.0   11.5
11        35.25   11.5
15         0.0   20.5
16        35.25   20.5
C ANGLE
C FASTENER BOLTS
```

```
29        1.51  11.5
30        1.51  14.5
31        1.51  17.5
32        1.51  20.5
C OUTSTANDING LEG
17       -0.75  10.0
20       -0.75  11.5
23       -0.75  20.5
26       -0.75  22.0
C OTHER NODES IN ANGLE FOR TOPOLOGICAL DESCRIPTION
19        3.25  10.0
22        3.25  11.5
25        3.25  20.5
28        3.25  22.0
33       -0.75  14.5
35       -0.75  17.5
38         1.51  10
39        1.51   22
C X- COORDINATE HAS TO BE CHANGED WITH EACH NEW THICKNESS
C X-COORD=-.75+THICK
36      -0.375 17.5
34      -0.375 14.5
27      -0.375 22.0
24      -0.375 20.5
21      -0.375 11.5
18      -0.375 10.0
C ADDITIONAL NODES FOR SPRING
C ATTACH TO SPRING AND GROUND.SPRING LENGTH=BOLT GRIP LENGTH
37      -1.625   11.5
40      -1.625   14.5
41      -1.625   17.5
42      -1.625   20.5
C ADD NODE FOR VIEW OF DISPLACED SHAPE
43       0      0     100000
ELEMENTS
ELEMENT.TYPE=30100
GROUP=1
PROP=4
NUMBER   TOPO
1        20  37
2        33  40
3        35  41
4        23  42
PAFBLOCKS
TYPE=1
ELEMS.ARE.8.NODE.QUADS=36210
GROUP       PROP       N1       N2       TOPOLOGY
C WEB
11          2          4        5        9  10 15 14
13          2          1        3        3  4  9  11
14          2          6        5        10 11 14 16
15          2          1        7        15 16 5  6
```

```
C ANGLE WEB ELEMENTS
5           4           13       10       18 38 21 29
6           4           13       12       21 29 24 32
7           4           13       15       24 32 27 39
8           4           14       10       38 19 29 22
9           4           14       12       29 22 32 25
10          4           14       15       32 25 39 28
PAFBLOCKS
TYPE=10
ELEMS.ARE.6.NODE.QUADS=36240
GROUP       PROP        N1       TOPOLOGY
C FLANGES
12          1           1        1  2  3  4
16          1           1        5  6  7  8
PAFBLOCKS
TYPE=1
ELEMS.ARE.8.NODE.QUADS=36210
GROUP       PROP        N1       N2       TOPOLOGY
C ANGLE COLUMN ELEMENTS
2           3           9        12       20 21 23 24
3           3           9        10       17 18 20 21
4           3           9        15       23 24 26 27
MESH.SPACING
REFER.TO.N1.OR.N2         SPACING.RATIO.OR.NO.OF.ELEM
1                         2  2  3  3  4  5  5  7  7  9
2                         1
3                         2
4                         1
5                         3
6                         2  3  3  4  5  5  7  7  9
7                         2
8                         1
9                         1
10                        2
12                        9
13                        3
14                        2
15                        2
MATERIALS
MATERIAL.NO       E          NU
1                 29E6       0.3
PLATES.AND.SHELLS
MATERIAL.NUMBER=1
PLATE.NUMBER        THICKNESS
1                   3.5
2                   0.1875
3                   2.0
C THICKNESS TO BE CHANGED
4                   0.375
SPRINGS
NUMBER.OF.SPRINGS        KX
4                         5.049E5
```

```
STRESS.ELEMENTS
GROUP
1
2
3
4
5
6
7
8
9
10
DISPLACEMENTS.PRESCRIBED
NODE   DIRE   DISP.VALU   LOAD.CASE
2      2       0.02300     1
REPEATED.FREEDOMS
DIRE=12
N1   N2
10   29
12   30
13   31
14   32
GRAPH.OF.DISPLACEMENTS
TYPE   LIST.OF.NODES
C  X-DISP ALONG X=0
1      1    7
C  X DISP ALONG X=-0.25
1      18   27
C  Y DISP OF LOWER FLANGE
2      1    2
C  X DISP ALONG X=0 JUST BENEATH ANGLE
1      9    15
RESTRAINTS
NODE   PLANE   DIRE
C  ADD NODES TIED TO SPRINGS
37     0       0
40     0       0
41     0       0
42      0       0
C TREAT BOTTOM BOLT AS A HORIZONTAL ROLLER
20     0       2
C  RESTRAIN TO PLANE PROBLEM
1      3       3456
OUT.DRAW
DRAW    PLOT    NODE
1       1       43
2       20
REACTIONS
C  REPLACE REACTIONS IN C M TO ONLY ACTIVE NODES
C  IE AT CONSTRAINTS AND AT PRES DISPS
NODES
2
20
```

```
23
37
40
41
42
SELECT.DRAW
DRAW   ELEM   TYPE   N1   N2   N3
2      36210  1      17   26   19
END.OF.DATA
```

For Quarter-Inch Angle Thickness

```
CONTROL
NAME.T250
FAST.READ
FULL.CONTROL
PHASE=1
PHASE=2
PHASE=4
PHASE=6
BASE=27500
SAVE
SAVE.FILES
PHASE=7
BASE=38000
SAVE.FILES
SAVE.DISPS
PHASE=8
BASE=38000
PHASE=9
BASE=38000
PHASE=10
BASE=38000
CONTROL.END
TITLE MOM CAP OF STD CLIP L CONN   , T=.25,JUL 24/80
NODES
NODE      X      Y      Z
C W-SECTION
C LOWER FLANGE
1          0.0    0.0
C NODE FOR LOAD APPLICATION,CUTTING LAST SEGMENT OF BEAM
2         35.25    0.0
3          0.0    0.5
4         35.25    0.5
C UPPER FLANGE
5          0.0   23.0
6         35.25   23.0
7          0.0   23.5
8         35.25   23.5
C ROW OF FASTENER BOLTS
10         1.50   11.5
12         1.50   14.5
13         1.50   17.5
14         1.5    20.5
C OTHER NODES IN WEB FOR TOPOLOGICAL DESCRIPTION
9          0.0   11.5
11        35.25   11.5
15         0.0   20.5
16        35.25   20.5
```

```
C ANGLE
C FASTENER BOLTS
29        1.51  11.5
30        1.51  14.5
31        1.51  17.5
32        1.51  20.5
C OUTSTANDING LEG
17       -0.75  10.0
20       -0.75  11.5
23       -0.75  20.5
26       -0.75  22.0
C OTHER NODES IN ANGLE FOR TOPOLOGICAL DESCRIPTION
19        3.25  10.0
22        3.25  11.5
25        3.25  20.5
28        3.25  22.0
33       -0.75  14.5
35       -0.75  17.5
38         1.51  10
39        1.51   22
C X- COORDINATE HAS TO BE CHANGED WITH EACH NEW THICKNESS
C X-COORD=-.75+THICK
36      -0.500 17.5
34      -0.500 14.5
27      -0.500 22.0
24      -0.500 20.5
21      -0.500 11.5
18      -0.500 10.0
C ADDITIONAL NODES FOR SPRINGS
C ATTACH TO SPRING AND GROUND.SPRING LENGTH=BOLT GRIP LENGTH
37      -1.50  11.5
40      -1.50  14.5
41      -1.50  17.5
42      -1.50  20.5
C ADD NODE FOR VIEW OF DISPLACED SHAPE
43      0      0     100000
ELEMENTS
ELEMENT.TYPE=30100
GROUP=1
PROP=4
NUMBER   TOPO
1       20  37
2       33  40
3       35  41
4       23  42
PAFBLOCKS
TYPE=1
ELEMS.ARE.8.NODE.QUADS=36210
GROUP      PROP      N1      N2      TOPOLOGY
C WEB
11         2         4       5       9  10 15 14
13         2         1       3       3  4  9  11
14         2         6       5       10 11 14 16
15         2         1       7       15 16 5  6
```

```
C ANGLE WEB ELEMENTS
5          4          13        10        18 38 21 29
6          4          13        12        21 29 24 32
7          4          13        15        24 32 27 39
8          4          14        10        38 19 29 22
9          4          14        12        29 22 32 25
10         4          14        15        32 25 39 28
PAFBLOCKS
TYPE=10
ELEMS.ARE.6.NODE.QUADS=36240
GROUP      PROP       N1        TOPOLOGY
C FLANGES
12         1          1         1  2  3  4
16         1          1         5  6  7  8
PAFBLOCKS
TYPE=1
ELEMS.ARE.8.NODE.QUADS=36210
GROUP      PROP       N1        N2        TOPOLOGY
C ANGLE COLUMN ELEMENTS
2          3          9         12        20 21 23 24
3          3          9         10        17 18 20 21
4          3          9         15        23 24 26 27
MESH.SPACING
REFER.TO.N1.OR.N2          SPACING.RATIO.OR.NO.OF.ELEM
1                          2  2  3  3  4  5  5  7  7  9
2                          1
3                          2
4                          1
5                          3
6                          2  3  3  4  5  5  7  7  9
7                          2
8                          1
9                          1
10                         2
12                         9
13                         3
14                         2
15                         2
MATERIALS
MATERIAL.NO      E          NU
1                29E6       0.3
PLATES.AND.SHELLS
MATERIAL.NUMBER=1
PLATE.NUMBER      THICKNESS
1                 3.5
2                 0.1875
3                 2.0
C THICKNESS TO BE CHANGED
4                 0.250
SPRINGS
NUMBER.OF.SPRINGS      KX
4                       1.405E5
```

```
STRESS.ELEMENTS
GROUP
1
2
3
4
5
6
7
8
9
10
DISPLACEMENTS.PRESCRIBED
NODE    DIRE    DISP.VALU    LOAD.CASE
2       2       0.04600      1
REPEATED.FREEDOMS
DIRE=12
N1    N2
10    29
12    30
13    31
14    32
GRAPH.OF.DISPLACEMENTS
TYPE    LIST.OF.NODES
C  X-DISP ALONG X=0
1       1    7
C  X DISP ALONG X=-0.25
1       18   27
C  Y DISP OF LOWER FLANGE
2       1    2
C  X DISP ALONG X=0 JUST BENEATH ANGLE
1       9    15
RESTRAINTS
NODE    PLANE    DIRE
C  ADD NODES TIED TO SPRINGS
37      0        0
40      0        0
41      0        0
42      0        0
C TREAT BOTTOM BOLT AS A HORIZONTAL ROLLER
20      0        2
C  RESTRAIN TO PLANE PROBLEM
1       3        3456
OUT.DRAW
DRAW     PLOT     NODE     GROUP
1        1        43       0
2        20                2 3 4 5 6 7 8 9 10
REACTIONS
C  REPLACE REACTIONS IN C M TO ONLY ACTIVE NODES
C  IE AT CONSTRAINTS AND AT PRES DISPS
```

```
NODES
2
20
23
37
40
41
42
END.OF.DATA
```

VITA

Abdallah J. Jubran was born in Beirut, Lebanon, on January 19, 1954. He attended elementary and high schools in that city and was graduated from International College in 1974 with a Part II Lebanese Baccalaureate in Mathematics. In September of 1975 he entered The University of Tennessee, Knoxville, and in June of 1978 he received a Bachelor of Science degree in Civil Engineering.

In September of 1978, Mr. Jubran entered the Graduate School of The University of Tennessee, Knoxville, as a full-time student. He received the Master of Engineering degree with a major in Civil Engineering in June of 1981.

The author is a member of The American Concrete Institute as well as the Society of Engineering Science, and is an Engineer-in-Training in the State of Tennessee. Mr. Jubran is currently enrolled in the doctoral program in the Department of Engineering Science and Mechanics, The University of Tennessee, Knoxville.